THE MODEL LIFETIMES, BAND INTENSITIES, GROWTH SCENARIOS AND ATMOSPHERIC IMPLICATIONS OF SUBSTITUTE CHLOROFLUOROCARBONS

by
Kevin Robert Gurney

B.A. University of California, Berkeley
(1986)

SUBMITTED TO THE CENTER FOR METEOROLOGY
AND PHYSICAL OCEANOGRAPHY,
DEPARTMENT OF EARTH, ATMOSPHERIC, AND PLANETARY SCIENCES
IN PARTIAL FULFILLMENT OF THE
REQUIREMENTS FOR THE DEGREE OF

MASTER OF SCIENCE

at the

MASSACHUSETTS INSTITUTE OF TECHNOLOGY

February 1990

Signature of Author _____
Center for Meteorology and Physical Oceanography,
Dept. of Earth, Atmospheric and Planetary Science

Certified by _____
Ronald G. Prinn,
Thesis Supervisor

Accepted by _____
Chairman, Departmental Committee on Graduate Students

ABSTRACT

With the aid of a 1-D eddy diffusion, steady-state, chemical-dynamical model and an FT-IR spectrometer, the steady-state lifetimes, vertical distributions and band intensities of substitute CFC's have been investigated. The lifetimes of the substitutes are distinctly shorter than the CFC's they have been proposed to replace, CF_2Cl_2 and $CFCl_3$, and therefore are expected to have lower total amounts in the atmosphere for the same emissions once they are introduced. In addition, the main sink for these compounds is in the troposphere instead of the stratosphere, which is the case for the CFC's, implying less penetration into the stratosphere and greatly reduced ozone depletion for the same emissions. Measurement of the CH_2FCF_3 and $CHCl_2CF_3$ band intensities coupled with atmospheric burden scenarios imply a role for CH_2FCF_3 in the greenhouse effect.

TABLE OF CONTENTS

LIST OF TABLES

LIST OF FIGURES

1. INTRODUCTION

The emission of chlorinated fluorocarbons or "CFC's" into the atmosphere has been of considerable concern since they were first identified as compounds that lead to the catalytic destruction of ozone (Molina and Rowland, 1974). By photodissociation, and subsequent gas-phase reactions, odd chlorine is released whereby it serves as the catalyst in the removal of the ozone molecule. In addition, CFC's are strong absorbers of infrared radiation in the 10μm atmospheric window of the earth's emission spectrum and have been identified as potential contributors to the greenhouse problem; up to 16 percent of the total projected greenhouse forcing in the next century (Wang et. al., 1976, Hansen et. al., 1988).

Of primary concern amongst the many CFC's that exist are $CFCl_3$ (CFC-11) and CF_2Cl_2 (CFC-12) primarily because of their extensive production, use and long lifetimes in the atmosphere. The lifetimes of $CFCl_3$ and CF_2Cl_2 have been estimated at 74 ($^{+31}_{-17}$) and 111 ($^{+222}_{-44}$) years, respectively and the present atmospheric concentrations are approximately 250 pptv for $CFCl_3$ and 415 pptv for CF_2Cl_2 (Cunnold et. al., 1986).

These compounds have many industrial and manufacturing uses. $CFCl_3$ is used primarily as an aerosol propellant and as a blowing agent for plastic foam and foam insulation products. CF_2Cl_2 is used as an aerosol propellant and a refrigerant. The usefulness of these compounds coupled

with the desire of the lesser developed nations to acquire the conveniences associated with them suggests even higher future concentrations.

Measurements at remote locations on the globe have shown that the concentrations of these chemical species are indeed rising (Cunnold et. al., 1986). This observed trend, concern over global warming, and the convincing evidence of CFC involvement in the Antarctic Ozone Hole has led many countries to sign the Montreal Protocol which proposes to severely reduce the production of these two and other similar compounds (UNEP 1987, OTA-U.S. Congress 1988). As the world relies on these chemicals for so many applications, substitute compounds have been proposed that exhibit the useful aspects of $CFCl_3$ and CF_2Cl_2 but contribute less to the greenhouse problem and atmospheric ozone depletion. The principal compounds that have been proposed as replacements for $CFCl_3$ and CF_2Cl_2 are hydrogenated chlorofluorocarbons $CHCl_2CF_3$ (HCFC 123), CH_3CF_2Cl (HCFC 142b), $CHFClCF_3$ (HCFC 124), CH_2ClCF_2Cl (HCFC 132b), CH_3CFCl_2 (HCFC 141b), CHF_2Cl (HCFC 22), and hydrogenated fluorocarbons CH_2FCF_3 (HFC 134a), and CH_3CHF_2 (HFC 152a).

Because of their greater reactivity with the hydroxyl radical it is expected that these compounds will have lifetimes shorter than either $CFCl_3$ or CF_2Cl_2 and should be removed primarily in the troposphere. Hence, involvement in global warming and penetration into the stratosphere leading to ozone depletion would be reduced. In addition, the hydrogenated fluorocarbons (HFC-134a and HFC-152a) contain no chlorine, eliminating them as a threat to stratospheric ozone.

Anticipating the introduction of these compounds to the atmosphere, it is important to examine quantitatively their expected lifetimes and radiative properties. With the use of a one-dimensional steady-state model this thesis presents calculated model lifetimes and expected vertical distributions for these compounds and with the use of a Fourier transform infrared (FT-IR) spectrometer, this thesis also presents infrared band intensities for two of these compounds, CH_2FCF_3 and $CHCl_2CF_3$. In addition, growth scenarios based on the calculated lifetimes are presented and comparisons made between the substitute compounds and $CFCl_3$.

2. MODEL LIFETIMES AND VERTICAL DISTRIBUTION

Theory: To examine the distribution of a chemical species in an incompressible atmosphere, one starts with the continuity equation for the concentration of a chemical species *i*, where concentration is denoted by *[i]*. This is written as,

$$(1) \quad \partial[i]/\partial t = P_i - L_i - \nabla\bullet([i]\underline{v})$$

where P_i is the rate of production of *i*, L_i is the rate of destruction of *i* and $\underline{v}$ is the velocity vector (underbars denote vector quantities). For use in a one-dimensional model, (1) can be horizontally averaged yielding,

$$(2) \quad \partial\langle[i]\rangle/\partial t = \langle P_i - L_i\rangle - \partial\langle[i]w\rangle/\partial z$$

where <> represent a horizontal average. Using the mixing ratio *X* of species *i* defined as,

$$(3) \quad X_i = [i]/[m]$$

where *[m]* is the concentration of dry air, the second term on the right hand side of (2) can be written as,

$$(4) \quad \langle[i]w\rangle = \langle[m]wX_i\rangle.$$

Separation of w, X_i, and $[m]$ into mean and deviation quantities in the vertical, neglecting the covariance with $[m]'$, and demanding that the mean, horizontally averaged vertical velocity be zero yields for the second term on the right hand side of (2),

$$(5) \quad \langle [i]w \rangle = \langle [m] \rangle \langle w' X_i' \rangle .$$

Use of Prandtl mixing length theory (Appendix A) gives the continuity equation in mixing ratio formulation as,

$$(6) \quad \frac{\partial}{\partial t} \langle X_i \rangle = \frac{1}{[m]} \frac{\partial}{\partial z} \left(K_z \langle [m] \rangle \frac{\partial}{\partial z} \langle X_i \rangle \right) + \frac{\langle P_i - L_i \rangle}{[m]}$$

where K_z is the vertical eddy diffusion coefficient from Appendix A.

If one considers the chemical of concern to be in steady state and disallows any chemical sources in the atmosphere, the rate of destruction, L_i, can be defined as,

$$(7) \quad \langle L_i \rangle = \langle X_i [m] / \tau_i \rangle .$$

where τ_i is the chemical lifetime which will be defined later. Lastly, consider K_z constant in a given atmospheric layer, and define $[m]$ as (horizontal averaging is assumed but not explicitly stated from here on),

$$(8) \quad [m] = [m]_o \exp(-z/H)$$

where H is the scale height. The resulting equation,

$$(9) \quad \partial^2 X_i/\partial z^2 - 1/H \; \partial X_i/\partial z - X_i/\tau_i K_z = 0$$

is a second-order differential equation that can be solved yielding,

$$(10) \quad X_i(z) = A \exp[r_1 z] + B \exp[r_2 z]$$

$$(11) \quad r_1 = [(1/4H^2 + 1/\tau_i k_z)^{1/2} + 1/2H]$$

$$r_2 = -[(1/4H^2 + 1/\tau_i k_z)^{1/2} - 1/2H].$$

The solution of this expression for discrete layers in the atmosphere is the intent of the 1-D model. The constants, A and B, can be explicitly calculated for each layer if the mixing ratio or the flux at the surface and at the top of the model atmosphere are fixed. The theoretical considerations are examined in Appendix B.

Two important terms can be elicited from this expression and are worth considering in detail. The quantity $4H^2/K_z$ is the time scale for transport. It can be thought of as the average time it takes a molecule to be transported through a layer. The other term to consider is, τ_i, which is the average chemical lifetime of i in a layer. More specifically, this is the time required for one e-folding of the concentration of i due to chemical reactions in a given layer. For instance, given a chemical reaction

$$(12) \quad AB + C \rightarrow A + BC$$

the time rate of change of the molecule *AB* is found to be,

(13) $\partial/\partial t[AB](t) = -a[AB](t)$

which yields the solution,

(14) $[AB](t) = [AB](0)\exp(-a/t)$.

where *a* is the rate of the reaction which is equal to the product of the concentration of the species *C* and the rate constant k. For bimolecular reactions the rate constant is given by kinetic theory as,

(15) $k = A \exp(-E_a/RT)$

where *T* is temperature, *R* is the ideal gas constant, E_a is the activation energy, and *A* is the pre-exponential factor which incorporates other terms such as the frequency of molecular collisions and the geometric requirements for the alignment of colliding molecules.

For unimolecular reactions, or photolysis in the case of the chemical species considered here, the rate constant, J_i, is defined in a non-scattering atmosphere as,

(16) $$J_i = \int_0^\infty \sigma_i(\nu)\ I_\nu\ d\nu$$

where $\sigma_i(\nu)$ is the absorption cross section at frequency ν, and I_ν is the photon flux at frequency ν at a given height in the atmosphere. This is represented in a non-scattering atmosphere by Beer's law as,

$$(17) \quad I_v(z) = I_v(\infty) \exp\left\{ -\int_z^{\infty} \sum_j \sigma_j(\nu) [j] \cos\theta^{-1} dz' \right\}$$

where $\Sigma\sigma_j[j]$ is the total absorption coefficient due to all species, θ is the solar zenith angle and $I_v(\infty)$ is the radiation incident at the top of the atmosphere.

With the definitions of the reaction rate constants, one can explicitly define the chemical lifetime as a function of height,

$$(18) \quad \tau_i(z) = \left\{ \sum_n k_{in}(T) [n](z) + J_i(z) \right\}^{-1}$$

where $[n]$ is the concentration of the species that reacts with i. Table 1 gives the reactions and the rate constants for the substitute CFC's considered in this model as well as an additional compound, methylchloroform, whose use will be considered later.

As can be seen from equation (10), and as will be shown later on, it is the relative magnitude of $4H^2/K_z$ and τ_i that determine the vertical profile of a chemical species in the atmosphere. Given a vertical profile determined by (10), the total atmospheric lifetime of a species i in a layered model is defined as,

$$(19) \quad \tau_{i,atm} = \frac{\sum X_i [m] \Delta z}{\sum X_i [m] \tau_i(z)^{-1} \Delta z}.$$

where the summation is over the 37 layers in the model varying in thickness, Δz, from 1 Km to 5 Km.

The Model: The purpose of the one-dimensional model is to produce globally averaged lifetimes and vertical profiles of a chemical compound in a model atmosphere. The two primary assumptions and hence the greatest weaknesses of the 1-D model, are the assumption of spatial invariance in the x and y directions and the assumption that coefficients for vertical eddy diffusion can adequately describe vertical transport. The first assumption is clearly a poor one when considering the quantities necessary to determine lifetimes and vertical profiles. This limits the 1-D model to producing results that are global averages. The representative ability of the globally averaged results are only as robust as the representative ability of the globally averaged quantities necessary to produce the results, assuming that the mechanisms of chemical destruction are well measured and understood. The quantities necessary to produce the lifetimes and the vertical profiles are: the photodissociation rate constant, J; the rate constant of the reaction with the hydroxyl radical, k; the coefficient of vertical eddy diffusion, K_z; the particular substitute compound concentration; and the hydroxyl radical concentration, $[OH]$. I will consider each one of these quantities in turn.

The photodissociation rate constant depends on the absorption cross section of the particular substitute and the radiation in the absorbing frequency band at a given level in the atmosphere. The globally averaged lifetimes of the substitute CFC's are relatively insensitive to the

inclusion of photodissociation in the model due to the dominance of the reaction with tropospheric hydroxyl. To calculate the incident radiation at a given frequency and level in the atmosphere, use was made of annually averaged, vertical profiles of oxygen, ozone, and their absorption cross sections for 30 degrees north latitude in a non-scattering atmosphere (WMO vol. I, 1985). Incident radiation at the top of the atmosphere at 9:00 am (to simulate the diurnal average) and 30 degrees north latitude (to simulate the latitude average) was used to initiate the radiative code. The choice of 30 degrees north for these and the other profiles was that half the mass of the hemispheric atmosphere lies to either side of this latitude. References for the UV cross-sections are given in Table 1.

The rate constant of the reaction with the hydroxyl radical, k, is dependant upon temperature as shown in equation (15). The temperature profile used was an annually averaged, vertical profile from 30 degrees north latitude (U.S. Standard Atmosphere Supplements, 1966, and Stephen Fels, 1986). Two separate compendia of substitute-OH rate constants exist differing, in some cases, by a significant amount. Both have been considered in the model calculations and are listed in Table 1 along with the relevant reactions.

Three profiles of the vertical eddy diffusion coefficient, K_z, were used in the model as a test of the sensitivity of the lifetimes and profiles of the substitutes to K_z, and to adequately represent the range of K_z profiles presented in the literature (Chang, 1974, Hunten, 1975, Chang and Dickinson, 1975). These profiles are shown in Figure 1a.

Consideration of three K_z profiles helps us assess the adequacy of the second primary assumption noted above; the ability of K_z to account for vertical transport in the atmosphere. The values used were primarily calculated from experiments where the vertical distribution of a well-mixed chemical species such as methane, is modelled given known surface emissions and sinks in the atmosphere. From a measured distribution of the gas, the K_z profile is inferred (NAS, 1976). As will be shown, the atmospheric lifetime and the vertical profile of the substitutes prove insensitive to the range of K_z profiles considered here.

The substitute CFC's can be considered approximately horizontally well-mixed in the atmosphere if their lifetimes are greater than mixing times in the atmosphere. Of course, *a priori* knowledge of their lifetimes is necessary to assess this assumption which can be gleaned by examining the lifetime of a similar chemical species measured in the atmosphere, such as methylchloroform.

The horizontally averaged vertical profile of the hydroxyl radical is the most intransigent quantity to determine for input into the 1-D model. The hydroxyl radical is the primary oxidizing agent in the atmosphere and exhibits large spatial and temporal variance. In addition, the hydroxyl radical has not, as yet, been adequately measured. The approach used here to achieve a vertical profile of *OH* is the same used by Prinn et. al. (1987), utilizing data from the Atmospheric Lifetime Experiment/Global Atmospheric Gases Experiment (ALE/GAGE) (Prinn et. al., 1983). This approach uses the compound methylchloroform (CH_3CCl_3), whose global average lifetime can be

inferred from observations of concentration and known emissions ($<\tau_{mc}>$ = 6.3 $^{+1.2}_{-0.9}$ years), to determine the *OH* profile. Figure 1b shows the globally averaged *OH* profile adjustment necessary to achieve the 6.3 year global average lifetime for methylchloroform. This was performed by starting with a recent model calculated profile (Golombek and Prinn, 1986, WMO vol. II, 1985) and allowing the 1-D model to make adjustments by a constant factor in the troposphere until this lifetime is achieved. Figure 1c shows the normalized, global average, methylchloroform mixing ratio achieved with the 1-D model.

Model Results: Figures 2(a-j), 3(a-j), and 4(a-j) show the model results for the substitute CFC's in addition to results for $CFCl_3$ and CF_2Cl_2 using three different eddy diffusion coefficient profiles. As is evident from the figures, the global average lifetime of the substitutes is insensitive to the choice of the eddy diffusion coefficient profile, but the global average mixing ratio profile changes somewhat under these different transport schemes. The degree to which this is true depends upon the relative magnitude of the transport lifetime versus the chemical lifetime. At levels where the transport lifetime dominates or is equal to the chemical lifetime, the change in eddy diffusion coefficient results in a changed mixing ratio profile. The global average lifetimes of the two CFC's, CCl_3F and CCl_2F_2, are sensitive to the choice of transport coefficient as the flux into the stratosphere where destruction by photodissociation occurs, is critical to their atmospheric lifetime. The remaining results will use Hunten's, 1979 K_z profile. Table 2 lists the global average lifetime for each substitute under the two different OH rate constants.

Figure 5(a-j) shows the globally averaged, vertical profile of the destruction rate for the substitute CFC's as defined by equation (7). Unlike the traditional CFC's, the loss rate is greatest in the troposphere reflecting the combination of high substitute CFC concentrations and faster OH reaction rates. It is important to remember that the rate of destruction is derived from a normalized mixing ratio, therefore, comparison between compounds in these graphs can be misleading.

3. BAND INTENSITIES

Introduction: To achieve an estimate of the potential for substitute CFC's to be involved in atmospheric radiative trapping, the spectral location and band intensities of two available species, CH_2FCF_3 and $CHCl_2CF_3$, was investigated in collaboration with Dr. J. Elkins at NOAA/ERL using an FT-IR spectrometer with an unapodized resolution of 0.03 cm^{-1}. For CH_2FCF_3, this measurement was performed at two different temperatures, 220 K and 273 K and at seven different concentrations. In the case of $CHCl_2CF_3$, this measurement was performed at a temperature of 223 K and a single concentration. The measurements are in the process of completion (ie. five temperatures and seven concentrations for both gases). The results are preliminary and are unpublished. Due to incompatibility in data archiving formats, all spectral data reside at the NOAA/ERL laboratory and updated figures representing the following work are not available at this time.

Experimental: All infrared measurements were conducted using a Nicolet Model 7199 FT-IR spectrometer (Michelson interferometer) equipped with a KBr-Ge beamsplitter. The HgCdTe semiconductor detector was cooled to 77 K with liquid nitrogen. The sample compartment and optical bench of the spectrometer were enclosed together in a box, which was under a constant purge of dry nitrogen gas from a liquid nitrogen tank to reduce H_2O and CO_2 interferences in the spectra. Simultaneous interferograms of a white-light source and He-Ne laser provided a calibration scale accurate to $\pm$ 0.01 cm^{-1}.

The cylindrical IR gas cell with two concentric walls for insulation was constructed of stainless steel. The cross section for one end of the cell is shown in Figure 6. A vacuum was maintained between the two walls of the cell during the experiment to help ensure temperature stability. Ethanol from a bath cooled by a refrigerator with a double stage compressor was continuously passed through the cell. The lowest temperature for the gas cell with this system was 230 K. To achieve the lowest temperature of 220 K it was necessary to run two refrigerator units in parallel. Three platinum resistance thermometers were mounted inside the cell which were in direct contact with the gas. The temperature in the gas cell, inside the spectrometer, and in the room, and the pressure of the gas in the cell were continuously monitored using a Keithley digital voltmeter (DVM) and scanner. The resultant data were stored on discs using a Hewlett-Packard HP-85 computer. The temperature of the gas in the cell was maintained to ± 1 K at 297, 273, and 250 K and ± 2 K at 230 K and 220 K.

The IR windows attached to the inside wall were made of cesium iodide (CsI) and were sealed against the wall with viton o-rings. The inside wall of the cell was electropolished to reduce possible storage problems (Kagann et. al., 1983). The outside IR windows were made of potassium bromide (KBr) and were attached with RTV-silicon sealant. The length of the cold cell was fixed at 15.02 cm.

Nonlinearities in the detection of the IR signal in the FT-IR spectrometer can affect the band intensity measurement (Elkins et. al.,

1984). Photoconductive mercury cadmium telluride (PC-MCT) IR detectors are known to exhibit nonlinear responses in the presence of strong IR radiation. Detector nonlinearities can be reduced by placing either IR filters or screens between the detector and the IR source. Nonlinearities in the electronics used to amplify the IR signal can also affect the band intensity. The constant voltage amplifier built into the FT-IR spectrometer introduced nonlinearities to the spectrum. A constant current source preamplifier for the PC-MCT detector was used because this type of detector requires a constant current to perform properly (Elkins, manuscript in preparation).

Seven gas standards of CH_2FCF_3 and one of $CHCl_2CF_3$ in air were prepared in aluminum cylinders with stainless steel CGA-660 valves by gravimetric techniques which were accurate to ± 0.5 ppm. The mole fractions of the seven CH_2FCF_3 standards were 155.6, 194.8, 284.4, 455.0, 566.5, 733.6, and 976.7 parts per million (ppm) in air, respectively. The mole fraction of the single $CHCl_2CF_3$ standard was 148.8 ppm.

These gas standards provided a large supply of gas so that during the FT-IR analysis, a constant flow of the standard mixture could be passed through the gas cell. The flow rate was always maintained at 50 cc per minute. Pressurization of the cell was never encountered at this flow rate but was found to begin at flow rates of approximately 120 cc per minute. The same gas standard mixtures were used during the five constant temperature experiments.

All results are reported as partial pressure of substitute CFC at 296 K in order to eliminate confusion when intercomparing results. The total pressure of the gas mixture in the cell was accurately measured and was always about 630 torr. At low temperatures the number of molecules in the gas cell increases and the partial pressure of substitute CFC must be corrected according to the ideal gas law. Non-ideality of the gas mixture at low temperatures was also included in the correction. The partial pressure p of the substitute CFC in the cell is given by

$$(20) \quad p = \frac{296}{760} \frac{p_T}{T} \frac{Z(296)}{Z(T)} f$$

where P_T is the total pressure in mm of Hg (torr), T is temperature (degrees K), f is the mole fraction of the gas mixture and $Z(T)$ is the compressibility of air at temperature T and 1 atmosphere pressure (e.g. Z=0.99966 at 296 K and 1 atm).

Results: Figure 7a shows the absorption bands of CH_2FCF_3 between 1600 and 750 cm^{-1} at 223 K for the 198.4 ppm standard. Figure 7b shows the absorption bands of $CHCl_2CF_3$ between 1370 and 1050 cm^{-1} at 223 K for the 148.8 ppm standard.

Figure 8 shows the Beer's law plots of the log base 10 frequency integrated absorbance ($\int A_{10}\, dv$) versus the pressure-pathlength product for CH_2FCF_3 at 294 K for each of the six bands and the system. These figures illustrate the linearity of the band growth at these pressure-

pathlengths and this temperature. This is expected since all of the integrated absorbance measurements for CH_2FCF_3 were taken at optical depths of less than one, or less than 40% absorbance.

The band intensity S is calculated from

$$(21) \quad S = (pl)^{-1} \ln\{10^{(\int A_{10}\, d\nu)}\}.$$

where l is the cell length. Table 3 summarizes results for the two substitute compounds in addition to $CFCl_3$ and CF_2Cl_2, all corrected to 300 K.

Estimates of the uncertainties given in Table 3 were calculated by adding 2 major possible errors:

$$(22) \quad \varepsilon_{tot} = \varepsilon_r + \varepsilon_{sys}$$

where ε_r is the estimated random uncertainty in the integrated intensity and ε_{sys} is the estimated upper limit in the systematic error. The total random error was estimated by summing individual uncertainties in quadrature for pressure measurements, temperature fluctuations, impurities, pathlength measurements and the standard deviation in the determination of the slope of the Beer's law plot. The error estimate in pathlength was mostly due to the uncertainty in the correction for beam divergence in the gas cell. The estimate for a possible systematic error was based on comparing intensity values obtained by the present Fourier transform spectrometer with highly accurate values obtained by tunable

diode lasers and high resolution grating spectrometers (Kagann et. al., 1983, Kagann, 1982).

4. ATMOSPHERIC BURDEN SCENARIOS

Theory: Given the lifetimes of the substitute CFC's and some assumptions about the growth of emissions, future atmospheric burdens can be investigated. Rewriting (2) averaging in all directions gives,

$$(23)\quad \partial\langle M_i\rangle/\partial t = \langle E_i\rangle - \langle M_i/\tau\rangle$$

Where $\langle E_i\rangle$ is the globally averaged emission rate at the surface and M_i is the mass of gas i in the atmosphere. It can be expressed as (spatial averages are assumed from here on),

$$(24)\quad E_i = E_o \exp(rt)$$

where r is the annual, globally averaged rate of growth of the emission rate. Equation (23) can now be solved, yielding,

$$(25)\quad M_i(t) = E_o\ (\tau/(r\tau + 1))\ [\exp(rt) - \exp(-t/\tau)] + M_{io}\ \exp(-t/\tau)$$

where E_o and M_{io} are the initial emission rate and initial atmospheric burden, respectively.

The Model: To model the substitutes, I assume total conversion beginning in the year 1990 using the estimated 1990 emission rates of $CFCl_3$ as the initial emission rate. For $CFCl_3$, the 1980-1981 emission

rate was 265 x 10^9 grams/year (Chemical Manufacturers Association Reporting Company Data, Prinn, 1988). Using recent ALE/GAGE data through 1988 (Prinn et. al, 1983), (25) can be solved for the current emission growth rate. This calculation yields a 6% per year growth in the emission rate of $CFCl_3$. Using this emission growth rate, the initial emission rate for the substitutes in the year 1990 will be 421 x 10^9 g/year. To achieve a realistic growth in emissions over time, the growth rate will be assumed to decrease by 2% per year. The rate of emissions can then be expressed as,

$$(26) \quad E = E_o \exp[r_o e^{-.02\,t}\, t].$$

where t is time, and r_o is the initial rate of growth of emissions. To put approximate bounds on the model the above scenario will be run for initial percent emission growth rates ($100r_o$) of 5%, 7%, 10% and 15%.

Results: Figure 9(a-h) shows the results of the growth model. Included in the figures, where applicable, is the approximate present level of $CFCl_3$. In addition, the $CFCl_3$ mixing ratio assumed in a 1-D radiative-convective model run for greenhouse warming has been noted, where applicable, in the figure (Ramanathan et. al., 1985). This concentration, 1.0 ppb, contributed a 0.13 K surface warming out of a total 1.54 K surface warming which included all the known relevant radiatively active gases.

The emission scenarios run here are entirely speculative; the timing of the substitute CFC's introduction into manufacturing processes

and the subsequent growth in emissions is difficult to assess. Figure 9 shows four simple scenarios of which many are possible.

A measure of the substitute's impact on stratospheric ozone is the amount and height of odd chlorine release. In order to determine this in a fashion that allows intercomparison, an emission rate at the ground must be specified. The surface emission rate used was the level at which a given substitute compound reached steady-state in the atmosphere retrievable from the preceding calculations (using initial emission growth rate = 7%). By solving the system of equations in Appendix B with the flux at the ground fixed instead of the normalized mixing ratio, a vertical mixing ratio based on steady-state conditions can be calculated. The fractional amount of destruction of a compound, *i*, occurring in the stratosphere is expressed as,

$$(27) \quad f_{ssi} = \sum_{14}^{\infty} L_i \Big/ \sum_{0}^{\infty} L_i$$

where L_i is defined in equation (7). The fractional amount of substitute CFC odd chlorine release in the stratosphere relative to CFC-11, which will be termed the "chlorine release factor" (CRF), can then be expressed as,

$$(28) \quad CRF = f_{ssi}\, Cl\#_i \;/\; f_{ss11}\, Cl\#_{11}$$

where $Cl\#_i$ is the number of chlorines in a particular compound, and f_{ss11} is the fractional amount of CFC-11 destroyed in the stratosphere. Table

2 lists the *CRF* for each of the substitute compounds. This should not be compared to what is commonly referred to as the "ozone depletion potential" which is a measure of a compounds impact on stratospheric ozone per unit mass compared to the unit mass impact from CCl_3F (E.I. de Pont De Nemours & Company, Inc., 1988).

5. CONCLUSIONS

To qualitatively assess the "greenhouse potential" of the two substitute compounds for which band intensity measurements have been performed, the integrated band intensity and spectral distribution of these compounds relative to CCl_3F and CCl_2F_2 can be examined. As evidenced by Table 3, the integrated intensities of the two substitute compounds, CH_2FCF_3 and $CHCl_2CF_3$, are nearly equal to CCl_2F_2 and CCl_3F. Figure 10 shows the spectral location of the vibrational-rotational bands within the "window" region of the earth's atmosphere implying linear increases in absorption with increases in concentration. In other words, given the same atmospheric burden, these substitute compounds would exhibit approximately the same greenhouse potential as the traditional CFC's. For CH_2FCF_3, this is possible given the time series of atmospheric burden in figure 9 which shows CH_2FCF_3 reaching the present level of CCl_3F in the year 2020 under conservative emission rate growth.

With the exception of the totally fluorinated compounds, all of the substitutes can potentially deplete stratospheric ozone. The relative magnitude of this ability can be qualitatively assessed by examining Table 2. CH_3CFCl_2 has the largest "CRF" but an atmospheric lifetime shorter than both CH_3CF_2Cl and CHF_2Cl. It's relatively high chlorine release can be explained by the additional chlorine atom and the destruction rate versus height shown in figure 5. The relatively rapid decline in the destruction rate versus height in the troposphere

is a reflection of the strong temperature dependance of the OH rate constant. Such a decline allows a larger flux of a given substitute into the stratosphere. Next in magnitude of stratospheric chlorine release are $CHCl_2CF_3$ and $CH_2ClCClF_2$. While both of these compounds contain 2 chlorine atoms, $CH_2ClCClF_2$ exhibits a stronger OH rate constant temperature dependance meaning a larger stratospheric destruction rate than $CHCl_2CF_3$ and hence, a larger "CRF". The remaining substitutes, CH_3CF_2Cl, $CHFClCF_3$, and CHF_2Cl, have one chlorine and maintain relatively low destruction rates in the lower stratosphere resulting in the least stratospheric chlorine release.

The potential of the substitutes to destroy stratospheric ozone and contribute to global warming is also strongly dependant on the total atmospheric burden which is directly a function of the average atmospheric lifetime. The substitute compounds CH_3CCl_2F and $CH_2ClCClF_2$ which have the largest "CRF" are also compounds that could reach the present level of CCl_3F in the next 30 years under present growth rates. While such an analysis cannot claim to quantitatively assess the stratospheric ozone impact from the substitutes, it can place their relative importance to each other.

6. REFERENCES

Chang, J. S., *Proceedings of the Third CIAP Conference*, Rep. DOT-TSC-OST-74-15, 330-341, U.S. Dept. of Transportation, Washington, D. C., 1974.

Chang and Dickinson in National Academy of Sciences, *Halocarbons: Effects on Stratospheric Ozone*, National Academy of Sciences, Washington, D. C., 1976.

Cunnold, D. M., R. G. Prinn, R. A. Rasmussen, P. G. Simmonds, F. N. Alyea, C. A. Cardelino, A. J. Crawford, P. J. Fraser, and R. D. Rosen, *J. Geophys, Res.*, **91**, 10797-10817, 1986.

Elkins, J.W., R.H. Kagann, and R.L. Sams, *J. Molec. Spectrosc.* **105**, 480-490, (1984).

Elkins , J. W., and R. L. Sams, NBS Report, 553-K-86, 1986.

Elkins J. and J. Wen, manuscript in preparation, 1986.

Gillotay, D., P. C. Simon, and G. Brasseur, *Aeronomica Acta*, 340, 1989.

Golombek, A. and R. G. Prinn, *J. Geophys. Res.*, **91**, 3985-4001, 1986.

Golombek, A. and R. G. Prinn, *Geophys. Res. Lett.*, **16**, 1153-1156, 1989.

Hansen, J., I. Fung, A. Lacis, D. Rind, S. Lebedeff, R. Reudy, and G. Russell, *J. Geophys.Res.*, **93**, 9341-9364, 1988.

Hunten, D. M., *Proc. Nat. Acad. Sci., USA*, **72**, 4711-4715, 1975.

Kagann, R.H., J.W. Elkins, and R.L. Sams, *J. Geophys. Res.* **88**, 1427-1432, 1983.

Kagann R.H., *J. Molec Spectrosc.* **95**, 297-305, (1982).

Kurlyo, M. J., P. C. Anderson, and O. Klais, *Geophys. Res. Lett.*, **6**, 760-762, 1979.

Molina, M., J. and F. S. Rowland, *Nature*, **249**, 810-812, 1974.

National Academy of Sciences, *Halocarbons: Effects on Stratospheric Ozone*, National Academy of Sciences, Washington D. C., 1976.

National Aeronautics and Space Administration, *Chemical Kinetics and Photochemical Data for Use in Stratospheric Modeling*, JPL Publ. 87-41, 1987.

National Aeronautics and Space Administration, *Chemical Kinetics and Photochemical Data for Use in Stratospheric Modeling*, JPL unpublished manuscript, 1989.

Office of Technology Assessment, U. S. Congress, *An Analysis of the Montreal Protocol on Substances that Deplete the Ozone Layer*, February, 1988.

Prather, M. J., AFEAS Report 16, May, 1989.

Prinn, R., D. Cunnold, R. Rasmussen, P. Simmonds, F. Alyea, A. Crawford, P. Fraser, and R. Rosen, *Science*, **238**, 945-950, 1987.

Prinn, R. G., P. G. Simmonds, R. A. Rasmussen, R. D. Rosen, F. N. Aslyea, C. A. Cardelino, A. J. Crawford, D. M. Cunnold, P. J. Fraser, and J. E. Lovelock, *J. Geophys. Res*, **88**, 8353-8367, 1983.

Prinn, R. G., *The Changing Atmosphere*, 33-48, John Wiley & Sons Ltd., 1988.

Ramanathan, V., R. J. Cicerone, H. B. Singh, and J. T. Kiehl, *J. Geophys. Res.*, **90**, 5547-5566, 1985.

Simon, P. C., D. Gillotay, N. Vanlaethem-Meuree, and J. Wisemberg, *J. Atm. Chem.*, **7**, 107-135, 1988.

Stephen B. Fels, *Journal of the Atmospheric Sciences*, **43**, 219-221, 1986.

United Nations Environment Programme, *Montreal Protocol On Substances that Deplete the Ozone Layer*, 1987.

U.S. Standard Atmosphere Supplements, 1966, U.S. Government Printing Office, Washington D.C., 1966.

Wang, W. C., Y. L. Yung, A. A. Lacis, T. Mo, and J. E. Hansen, *Science*, **194**, 685-690, 1976.

World Meteorological Organization, Report No. 16, *Atmospheric Ozone 1985*, vol I, 1985.

World Meteorological Organization, Report No. 16, *Atmospheric Ozone 1985*, vol II, 1985.

APPENDIX A

Prandtl Mixing Length Theory: Consider a parcel of air which has an average characteristic quantity $\langle a \rangle$ associated with it. If the parcel moves a characteristic length, l' in the x direction before mixing with its surroundings, the difference between the quantity a in the new surroundings and that of the old can be expressed as,

$$(A1) \quad a' = \langle a \rangle(x_o) - \langle a \rangle(x_o + l')$$

where x_o is the initial position of the parcel (where $a = \langle a \rangle$). This can be given as,

$$(A2) \quad a' = \langle a \rangle(x_o) - (\langle a \rangle(x_o) + l' \, \partial\langle a \rangle/\partial x).$$

Which is,

$$(A3) \quad a' = -l' \, \partial\langle a \rangle/\partial x.$$

or more generally,

$$(A4) \quad a' = -l' \bullet \nabla\langle a \rangle.$$

This is the essence of Prandtl mixing length theory. The variance of a quantity associated with a parcel of air is equal to the product of the

characteristic distance it travels before mixing and the gradient of the average of the quantity. Consider equation (5) in chapter 2,

(A5) $\langle[i]\ w\rangle = \langle[m]\rangle\langle w' X_i'\rangle$.

Using mixing length theory this can be expressed as,

(A6) $\langle[i]\ w\rangle = -\langle[m]\rangle\langle w' l_z'\rangle \partial\langle X_i\rangle/\partial z$.

It is the covariance between w' and l_z' that is parameterized as the eddy diffusion coefficient, K_{zz}. This analysis can be extended to all three coordinate directions.

APPENDIX B

Calculating Coefficients, A and B: To calculate the coefficients, A and B, in equation (10) of chapter 2, one demands continuity of the concentration and the flux of a compound at each layer interface. This is expressed as,

$$(A1) \quad A_n \exp(r_{1n} \Delta z) + B_n \exp(r_{2n} \Delta z) = A_{n+1} + B_{n+1}$$

$$(A2) \quad K_{zn} [m]_n (\Delta z) (dX/dz)_n = K_{zn+1} [m]_{n+1} (0) (dX/dz)_{n+1}$$

where Δz is the thickness of layer n. By fixing the normalized mixing ratio or the flux at the surface and the top of the model atmosphere, a solvable system of equations is achieved. Fixing the normalized mixing ratios, these boundary conditions can be expressed as,

$$(A3) \quad X_1(z_1 = 0) = A_1 + B_1 = 1$$

$$(A4) \quad X_N(z_N = \Delta z) = A_N \exp(r_{1N} \Delta z) + B_N \exp(r_{2N} \Delta z) = 0$$

where N is the number of layers. The resultant system of equations consists of $2N-2$ equations and $2N-2$ unknowns. Gaussian elimination with pivotal condensation was used to solve the system.

Table 1. Reactions and Rate Constants

Num	Reaction	Rate constant JPL	Rate constant AFEAS
R1	$CH_3CCl_3 + OH \rightarrow CH_2CCl_3 + H_2O$	5.0e-12exp(-1800/T)[a]	5.0e-12exp(-1800/T)[b]
R2	$CH_2FCF_3 + OH \rightarrow CHFCF_3 + H_2O$	6.6e-13exp(-1300/T)[a]	1.7e-12exp(-1750/T)[b]
R3	$CHCl_2CF_3 + OH \rightarrow CCl_2CF_3 + H_2O$	1.1e-12exp(-1050/T)[a]	6.4e-13exp(-850/T)[b]
R4	$CH_3CF_2Cl + OH \rightarrow CH_2CF_2Cl + H_2O$	1.5e-12exp(-1800/T)[a]	9.6e-13exp(-1650/T)[b]
R5	$CH_3CHF_2 + OH \rightarrow$ products	1.9e-12exp(-1200/T)[a]	1.5e-12exp(-1100/T)[b]
R6	$CHFClCF_3 + OH \rightarrow CClFCF_3 + H_2O$	7.2e-13exp(-1250/T)[a]	6.6e-13exp(-1250/T)[b]
R7	$CH_2ClCClF_2 + OH \rightarrow CHClCClF_2 + H_2O$	3.4e-12exp(-1600/T)[a]	3.6e-12exp(-1600/T)[b]
R8	$CH_3CFCl_2 + OH \rightarrow CH_2CCl_2F + H_2O$	3.4e-12exp(-1800/T)[a]	2.7e-13exp(-1050/T)[b]
R9	$CHF_2Cl + OH \rightarrow CF_2Cl + H_2O$	8.3e-13exp(-1550/T)[a]	1.2e-12exp(-1650/T)[b]
R10	$CFCl_3 + OH \rightarrow$ products	1.0e-12exp(-3700/T)[a]	
R11	$CF_2Cl_2 + OH \rightarrow$ products	1.0e-12exp(-3600/T)[a]	
R12	$CH_3CCl_3 + h_\nu \rightarrow$ products	J_{12}[a]	
R13	$CH_2FCF_3 + h_\nu \rightarrow$ products	J_{13}[c]	
R14	$CHCl_2CF_3 + h_\nu \rightarrow$ products	J_{14}[d]	
R15	$CH_3CF_2Cl + h_\nu \rightarrow$ products	J_{15}[d]	
R16	$CH_3CHF_2 + h_\nu \rightarrow$ products	J_{16}[e]	
R17	$CHFClCF_3 + h_\nu \rightarrow$ products	J_{17}[a]	
R18	$CH_2ClCClF_2 + h_\nu \rightarrow$ products	J_{18}[f]	
R19	$CH_3CFCl_2 + h_\nu \rightarrow$ products	J_{19}[d]	
R20	$CHF_2Cl + h_\nu \rightarrow$ products	J_{20}[g]	
R21	$CFCl_3 + h_\nu \rightarrow$ products	J_{21}[g]	
R22	$CF_2Cl_2 + h_\nu \rightarrow$ products	J_{22}[g]	

a. NASA, JPL publ. 87-41, 1987.
b. Prather, 1989.
c. CH_3CCl_3 cross-section used.
d. Gillotay, Simon, and Brasseur, 1989.
e. NASA, JPL publ., 1989.
f. CH_2FCF_3 cross-section used.
g. Simon et. al., 1989.

Table 2. Model Lifetimes and Chlorine Deposition.

Compound	Lifetime (years)		f_{ss}		Chlorine Release Factor	
	JPL	AFEAS	JPL	AFEAS	JPL	AFEAS
CH_2FCF_3 (HFC 134a)	7.5	13.8	0.076	0.119	0.0	0.0
$CHCl_2CF_3$ (HCFC 123)	1.9	1.6	0.033	0.035	0.022	0.023
CH_3CF_2Cl (HCFC 142b)	21.4	19.4	0.048	0.049	0.016	0.016
CH_3CHF_2 (HFC 152a)	2.0	1.7	0.029	0.030	0.0	0.0
$CHFClCF_3$ (HCFC 124)	6.1	6.6	0.046	0.048	0.015	0.016
$CH_2ClCClF_2$ (HCFC 132b)	4.6	4.4	0.048	0.046	0.032	0.031
CH_3CFCl_2 (HCFC 141b)	9.4	7.5	0.049	0.059	0.033	0.039
CHF_2Cl (HCFC 22)	16.1	16.1	0.042	0.039	0.014	0.013
$CFCl_3$ (CFC-11)	72.3	-	1.0	-	1.0	-
CF_2Cl_2 (CFC-12)	133.5	-	0.98	-	0.656	-

Table 3. Band Intensities of Two Substitute CFC's

Compound	Total intensity (cm^{-2} atm^{-1} at 296 K)	
CH_2FCF_3 (HCFC 134_a)	3190 ±50	a
CCl_2F_2 (CFC 12)	3315 ±48	b
$CHCl_2CF_3$ (HCFC 123)	2411 ±40	a
CCl_3F (CFC 11)	2450 ±37	b

a. Preliminary results from J. W. Elkins (NOAA) and Kevin Gurney (MIT), 1988.

b. Elkins and Sams, 1986.

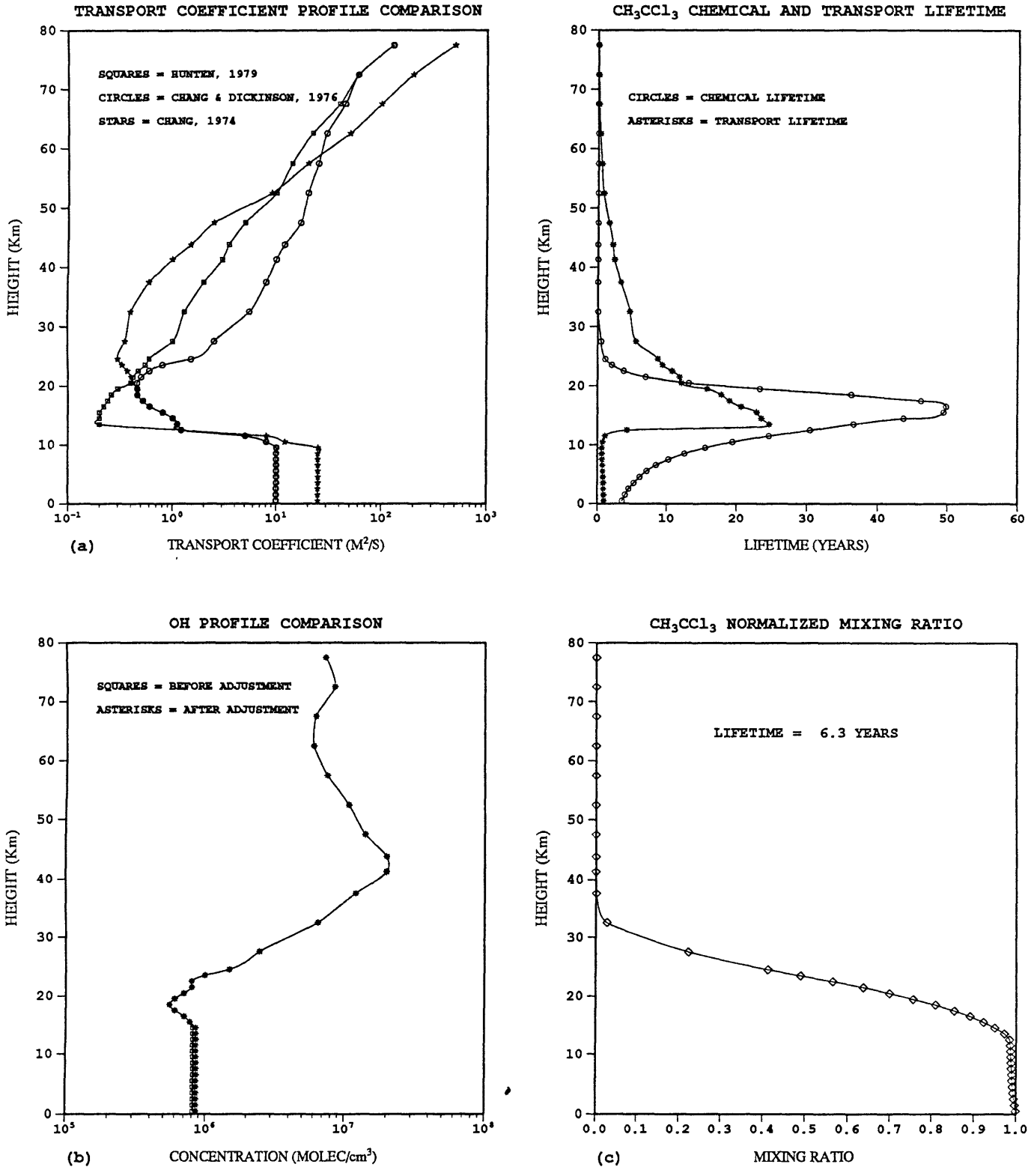

FIGURE 1: (a) Transport coefficient profile comparison. (b) OH concentration before and after adjustment. (c) Methylchloroform mixing ratio, chemical lifetime and transport lifetime.

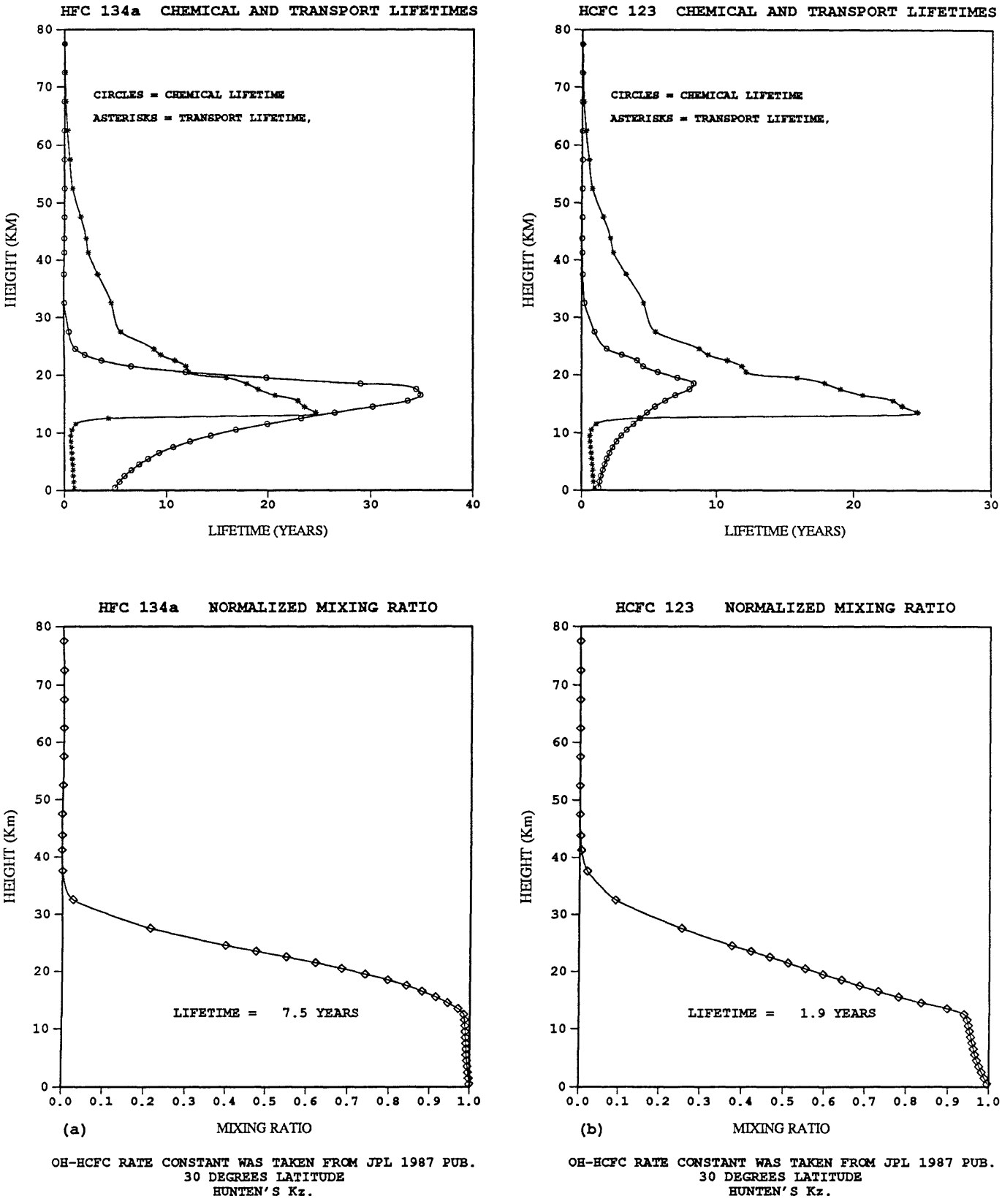

FIGURE 2: Model calculated vertical distribution, chemical lifetime and transport lifetime for the compounds listed.

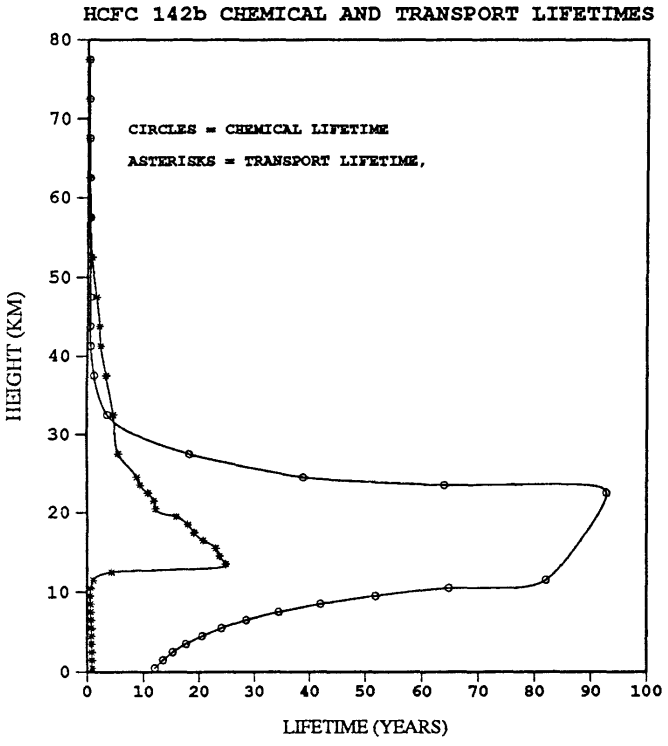

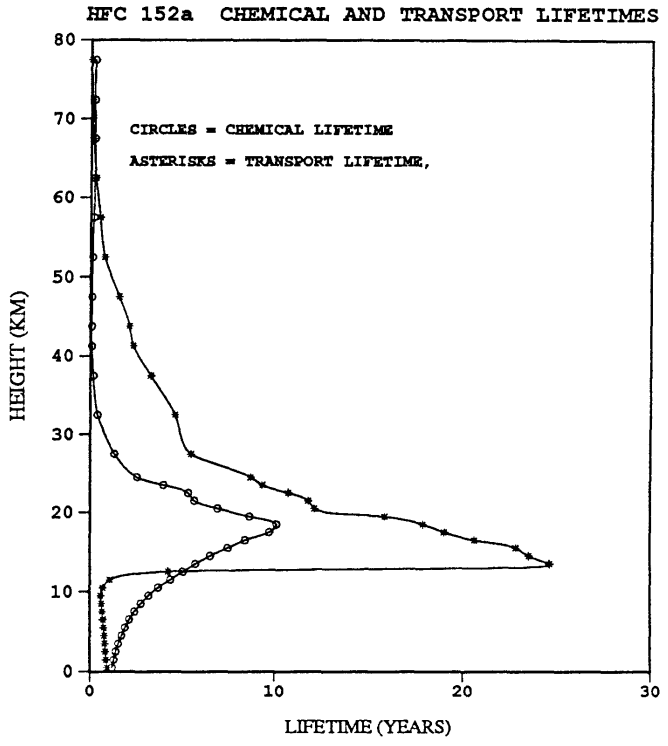

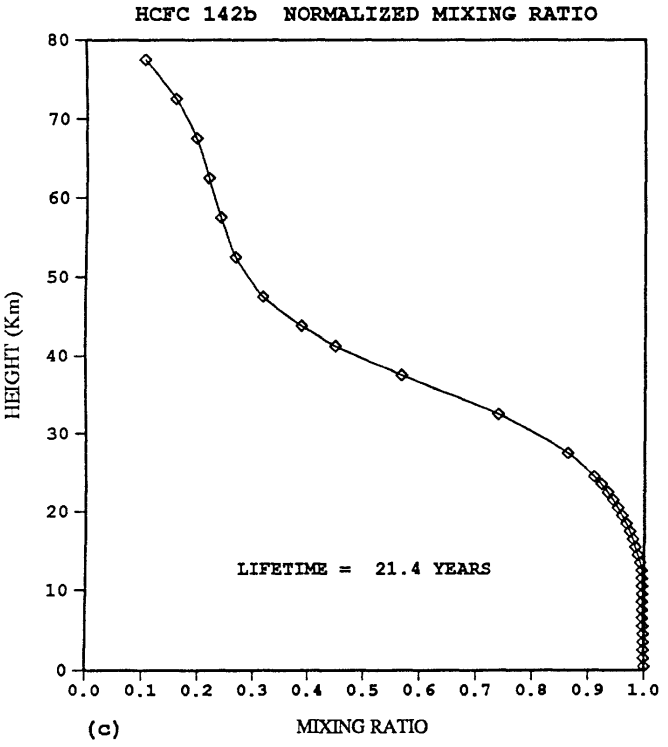

OH-HCFC RATE CONSTANT WAS TAKEN FROM JPL 1987 PUB.
30 DEGREES LATITUDE
HUNTEN'S Kz.

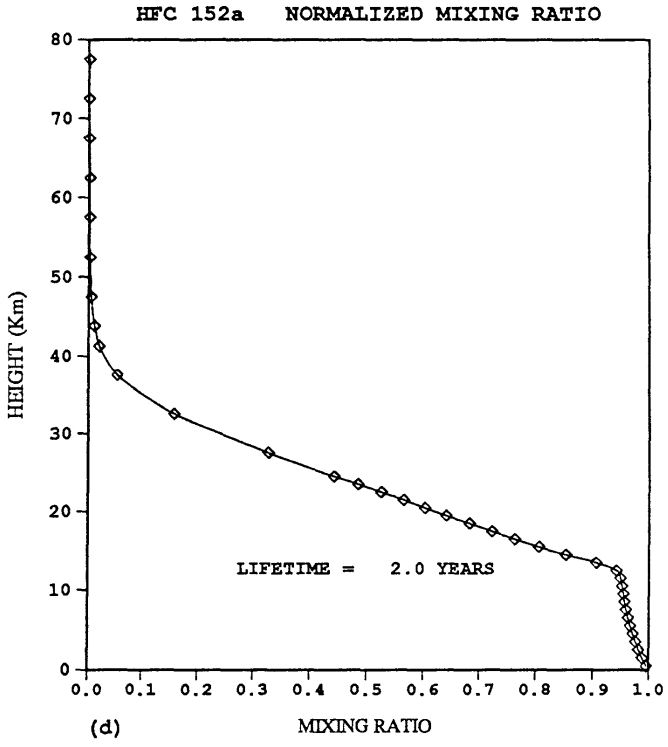

OH-HCFC RATE CONSTANT WAS TAKEN FROM JPL 1987 PUB.
30 DEGREES LATITUDE
HUNTEN'S Kz.

FIGURE 2: cont'd.

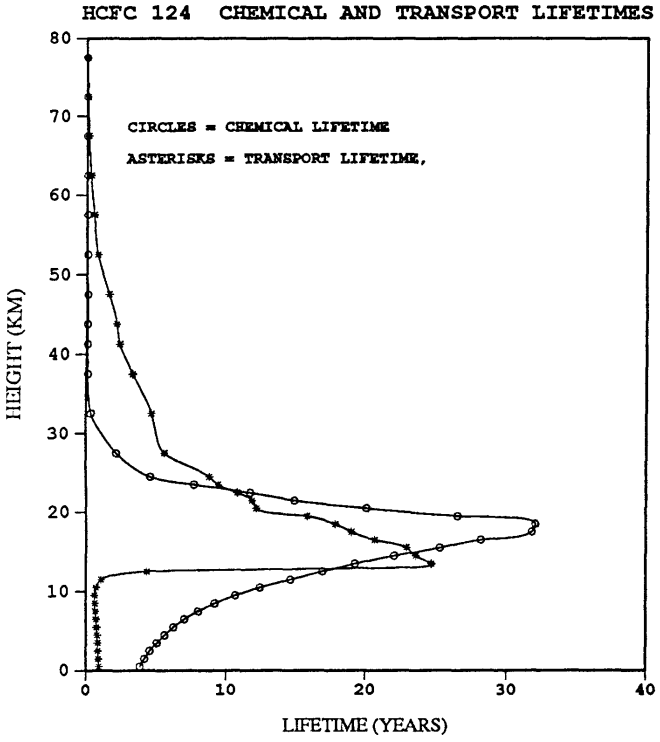

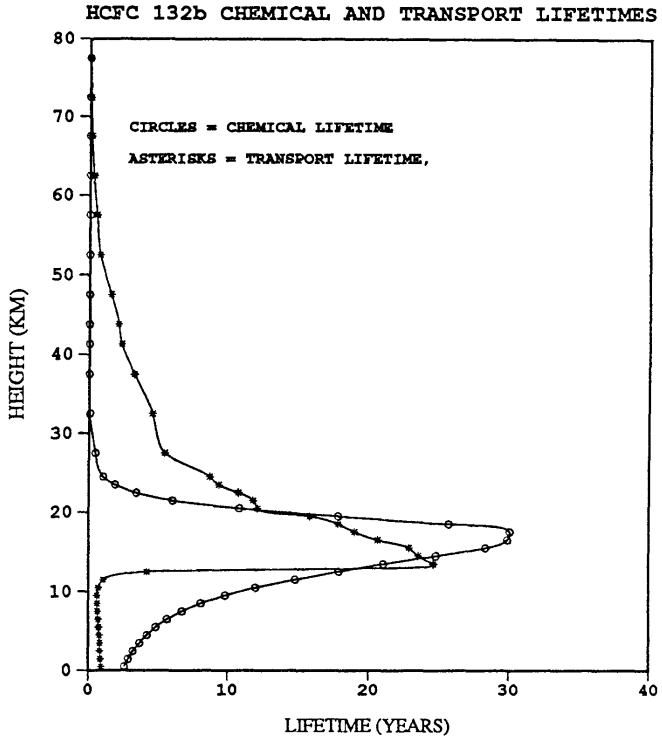

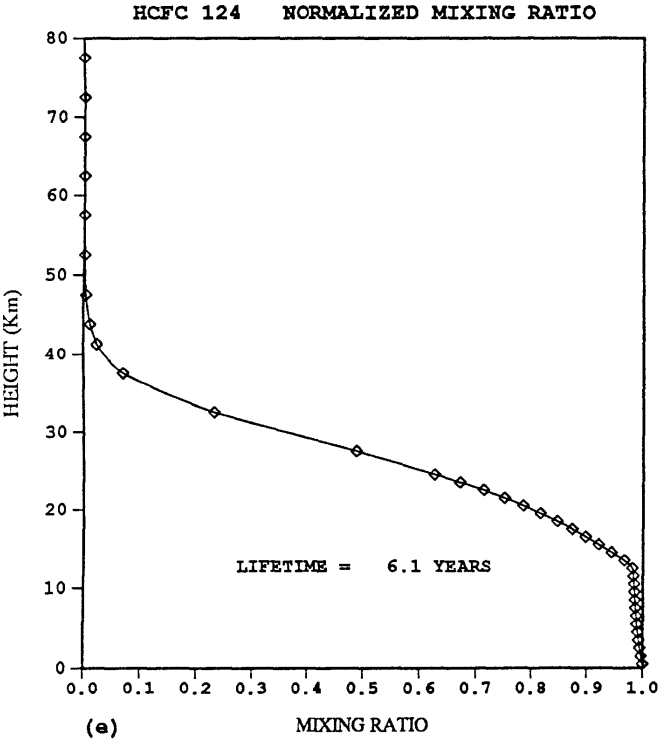

OH-HCFC RATE CONSTANT WAS TAKEN FROM JPL 1987 PUB.
30 DEGREES LATITUDE
HUNTEN'S Kz.

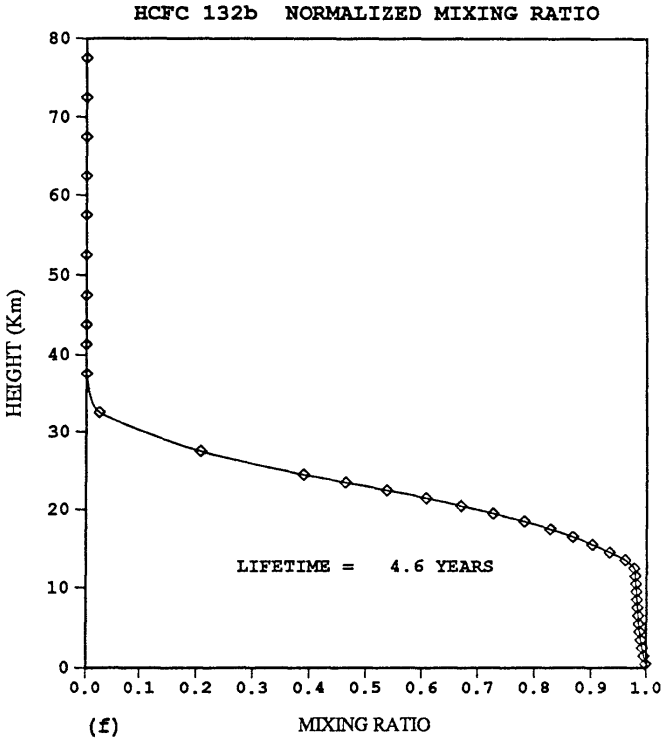

OH-HCFC RATE CONSTANT WAS TAKEN FROM JPL 1987 PUB.
30 DEGREES LATITUDE
HUNTEN'S Kz.

FIGURE 2: cont'd.

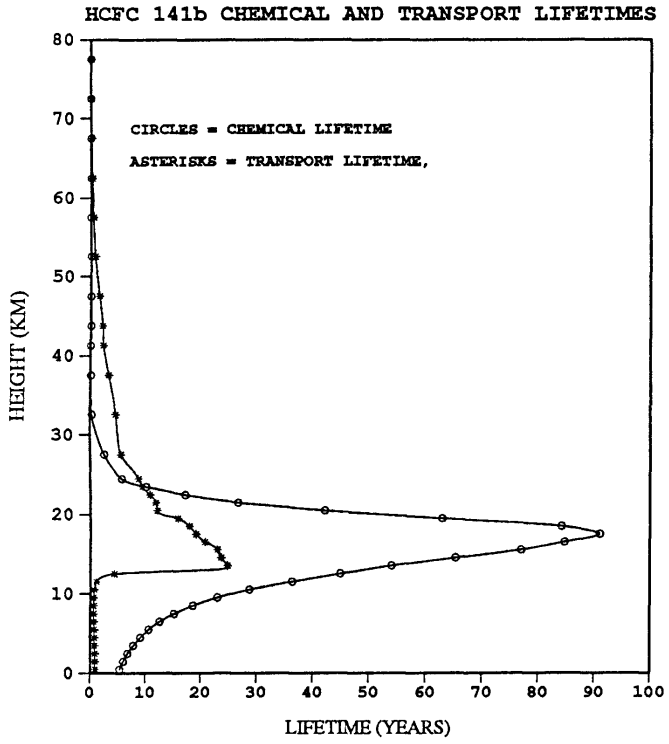

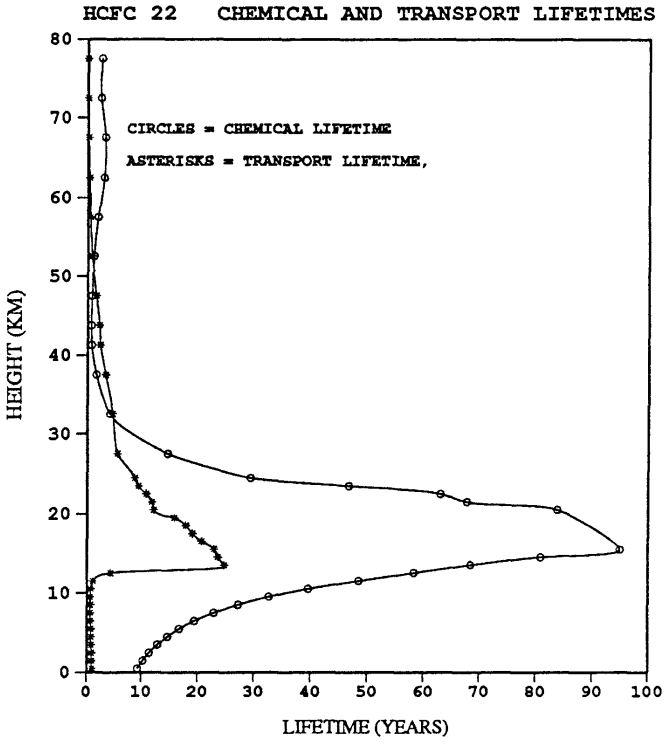

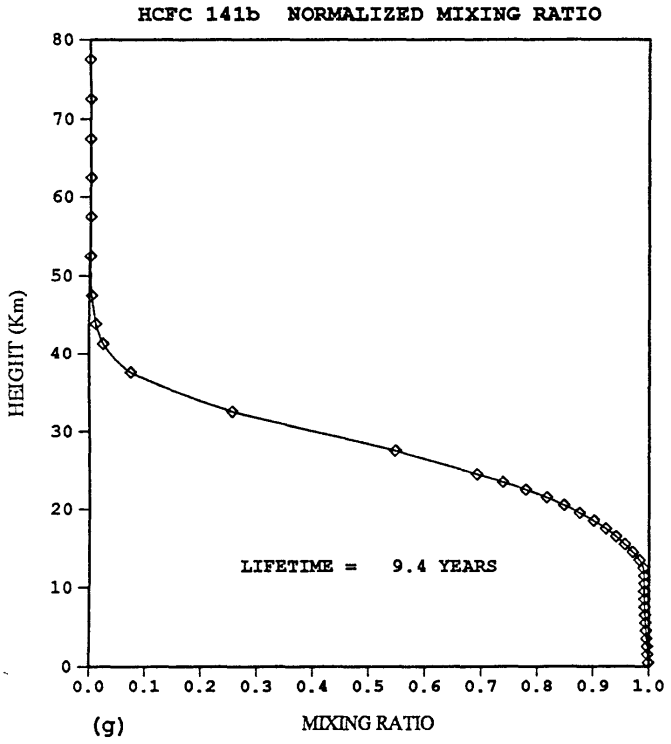

OH-HCFC RATE CONSTANT WAS TAKEN FROM JPL 1987 PUB.
30 DEGREES LATITUDE
HUNTEN'S Kz.

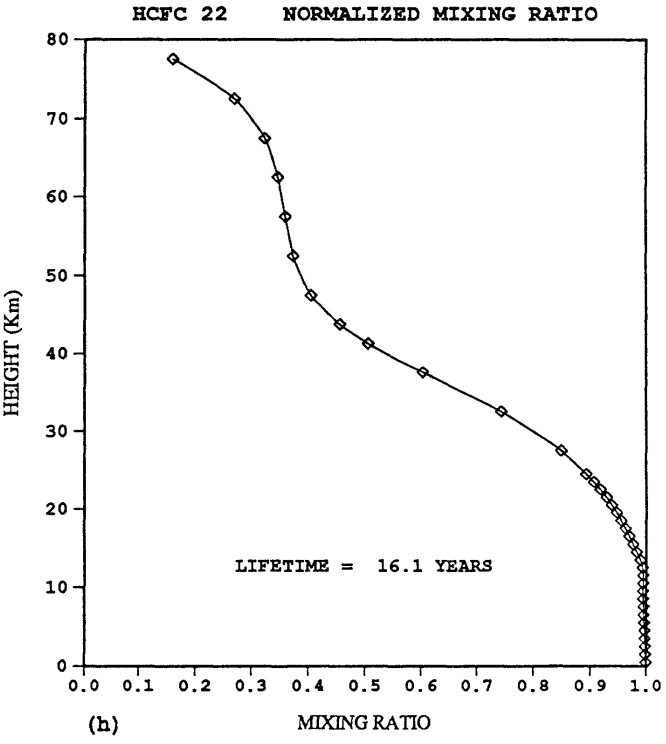

OH-HCFC RATE CONSTANT WAS TAKEN FROM JPL 1987 PUB.
30 DEGREES LATITUDE
HUNTEN'S Kz.

FIGURE 2: cont'd.

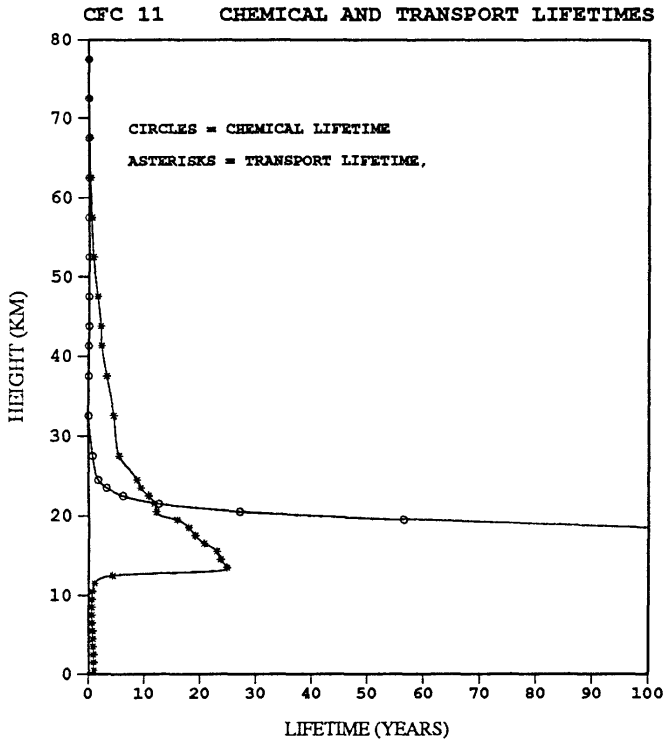

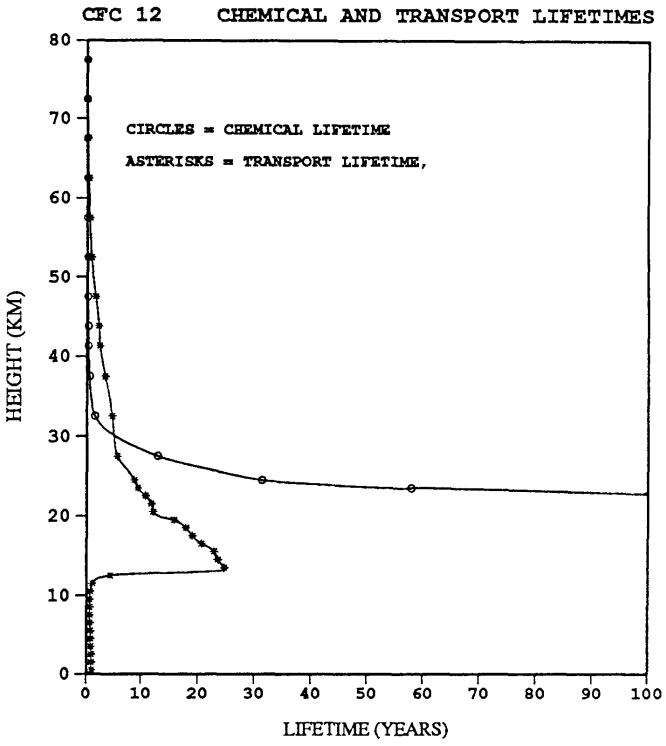

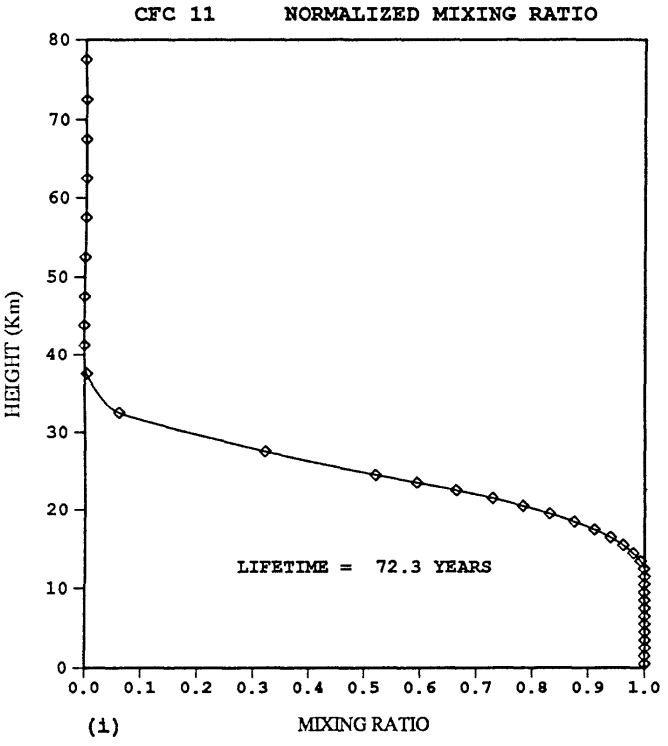

OH-HCFC RATE CONSTANT WAS TAKEN FROM JPL 1987 PUB.
30 DEGREES LATITUDE
HUNTEN'S Kz.

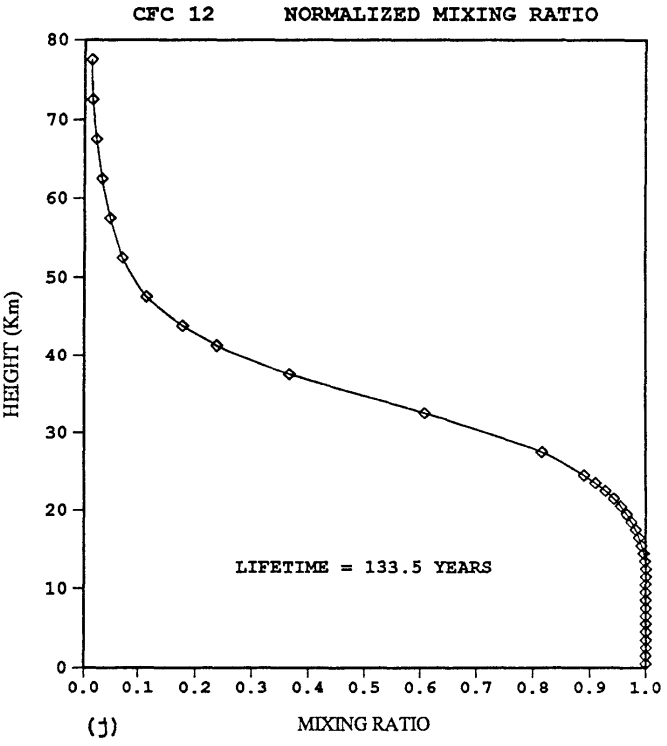

OH-HCFC RATE CONSTANT WAS TAKEN FROM JPL 1987 PUB.
30 DEGREES LATITUDE
HUNTEN'S Kz.

FIGURE 2: cont'd.

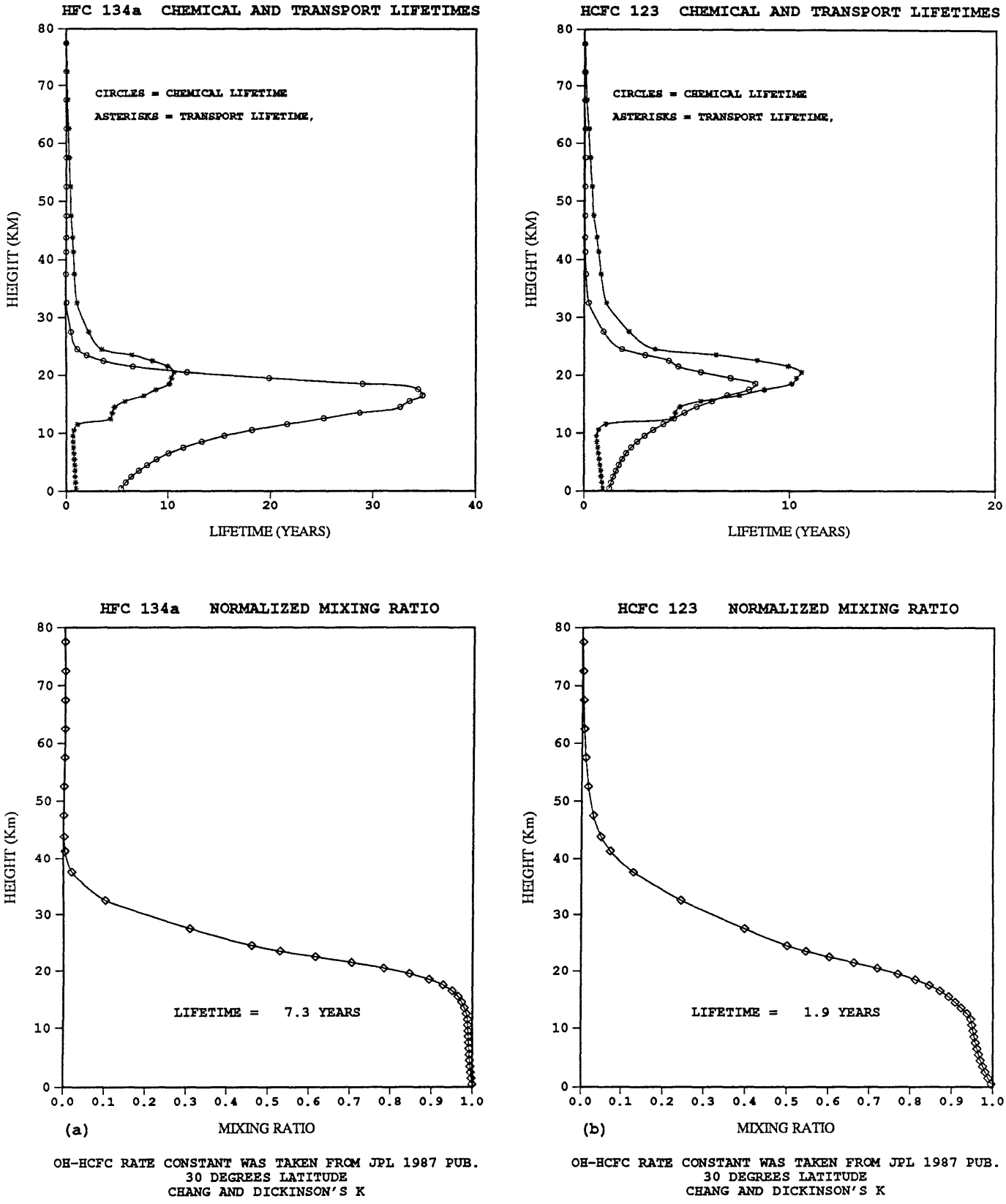

FIGURE 3: Same as in figure 2 but using the transport coefficient of Chang & Dickinson (1976).

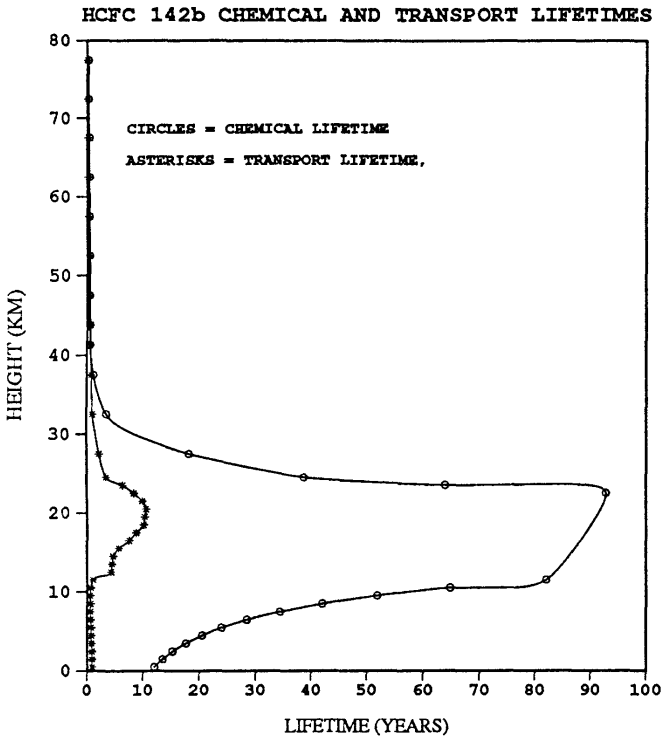

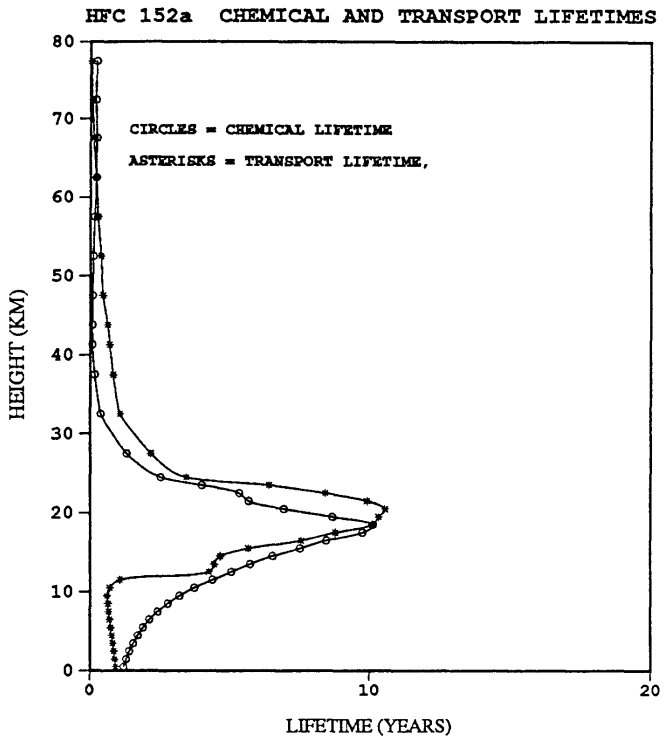

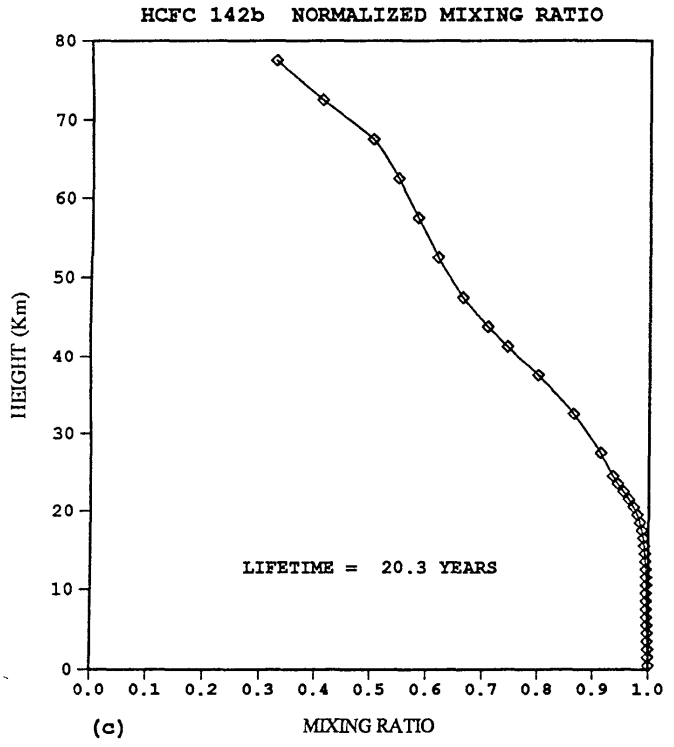

OH-HCFC RATE CONSTANT WAS TAKEN FROM JPL 1987 PUB.
30 DEGREES LATITUDE
CHANG AND DICKINSON'S K

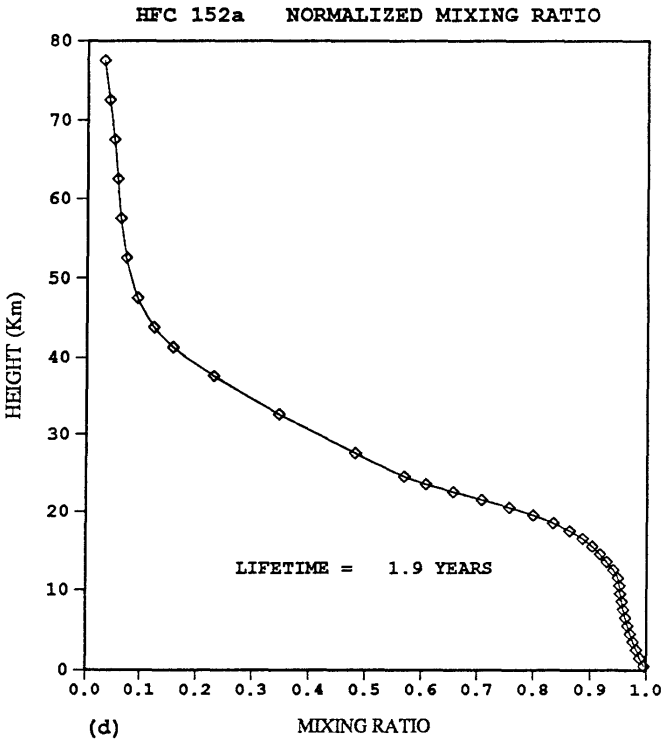

OH-HCFC RATE CONSTANT WAS TAKEN FROM JPL 1987 PUB.
30 DEGREES LATITUDE
CHANG AND DICKINSON'S K

FIGURE 3: cont'd.

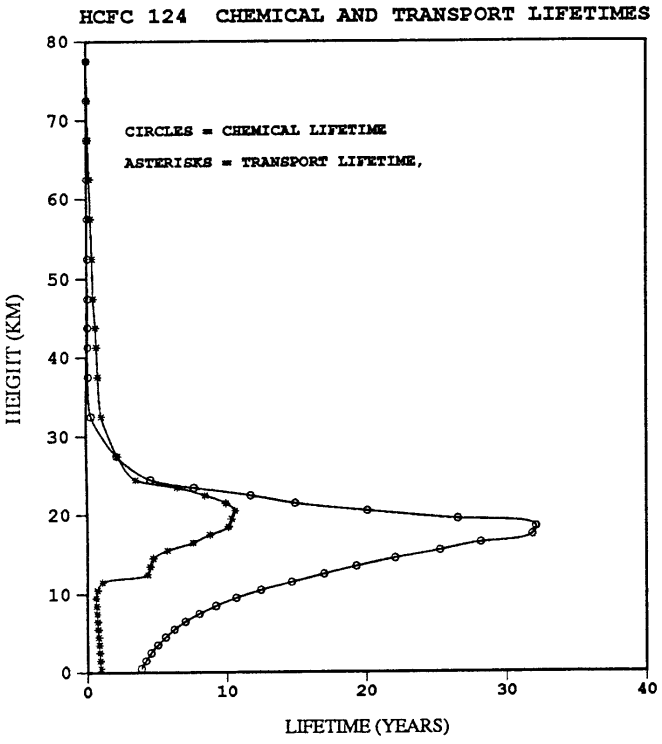

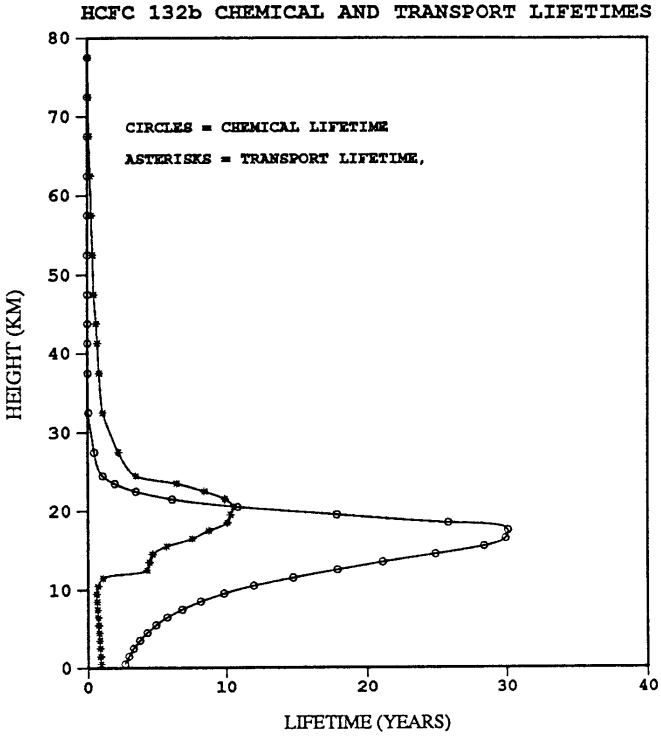

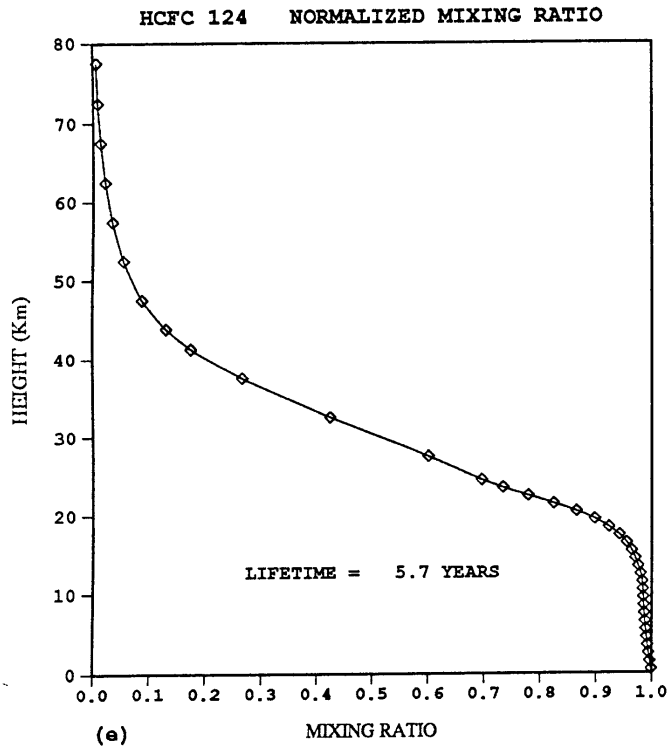

OH-HCFC RATE CONSTANT WAS TAKEN FROM JPL 1987 PUB.
30 DEGREES LATITUDE
CHANG AND DICKINSON'S K

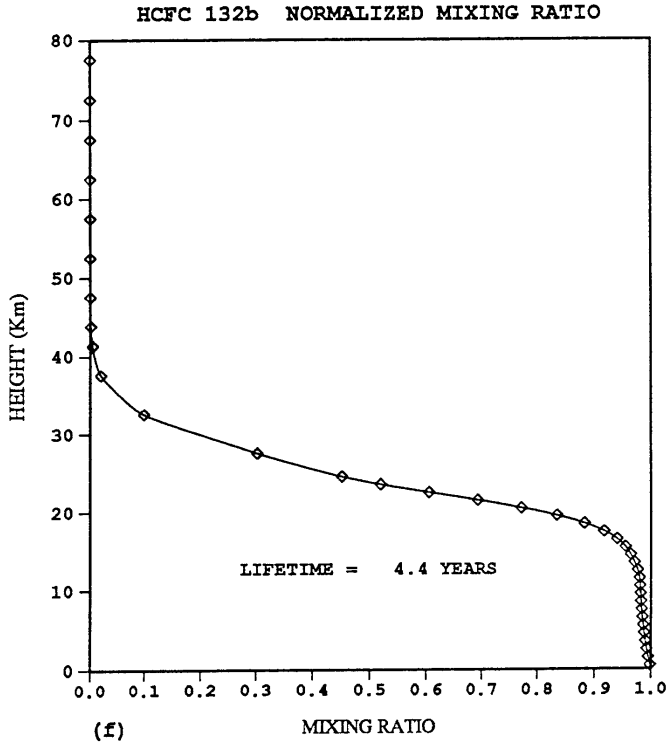

OH-HCFC RATE CONSTANT WAS TAKEN FROM JPL 1987 PUB.
30 DEGREES LATITUDE
CHANG AND DICKINSON'S K

FIGURE 3: cont'd.

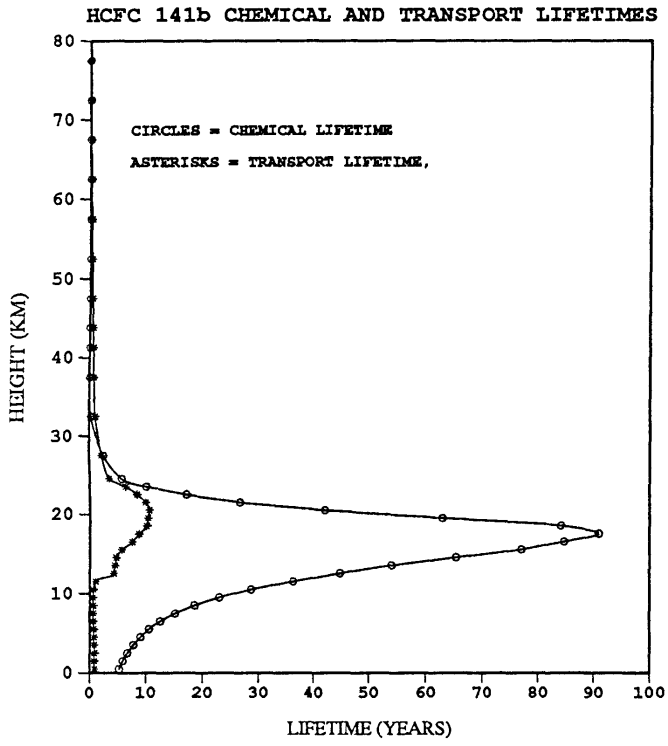

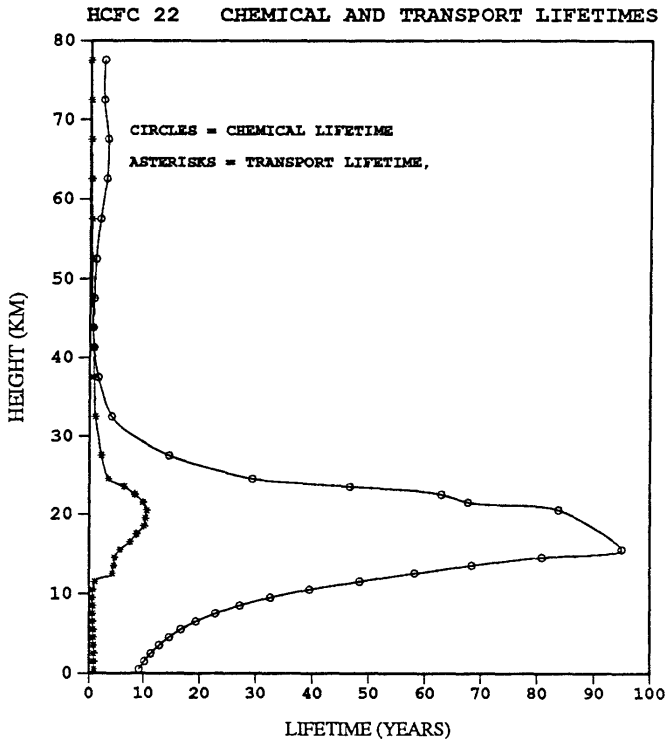

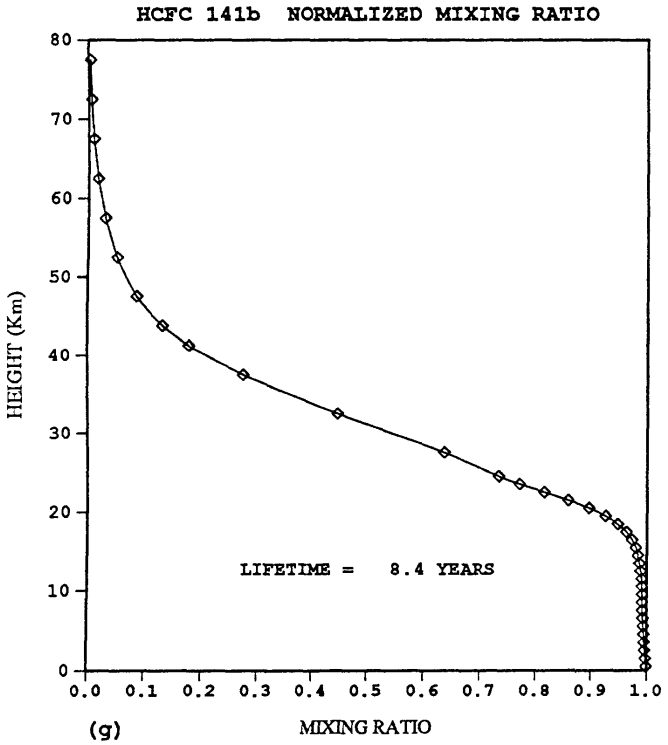

OH-HCFC RATE CONSTANT WAS TAKEN FROM JPL 1987 PUB.
30 DEGREES LATITUDE
CHANG AND DICKINSON'S K

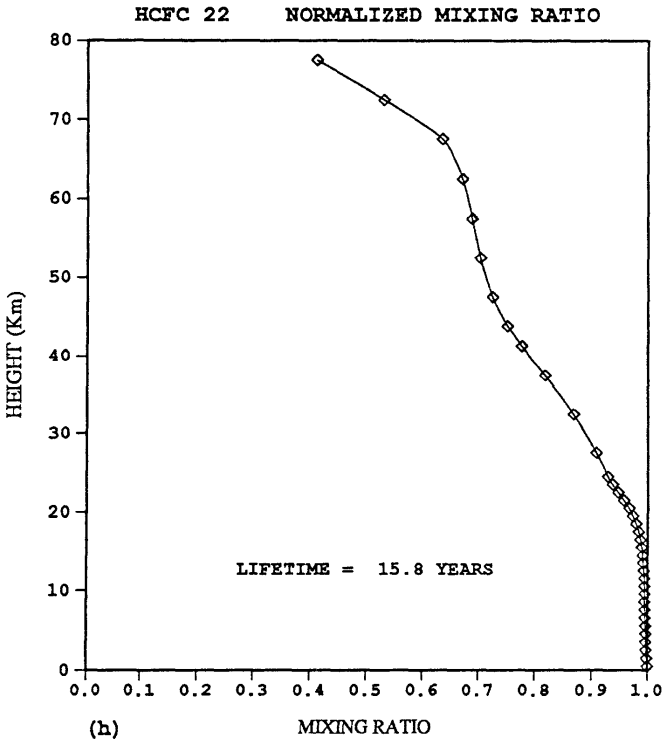

OH-HCFC RATE CONSTANT WAS TAKEN FROM JPL 1987 PUB.
30 DEGREES LATITUDE
CHANG AND DICKINSON'S K

FIGURE 3: cont'd.

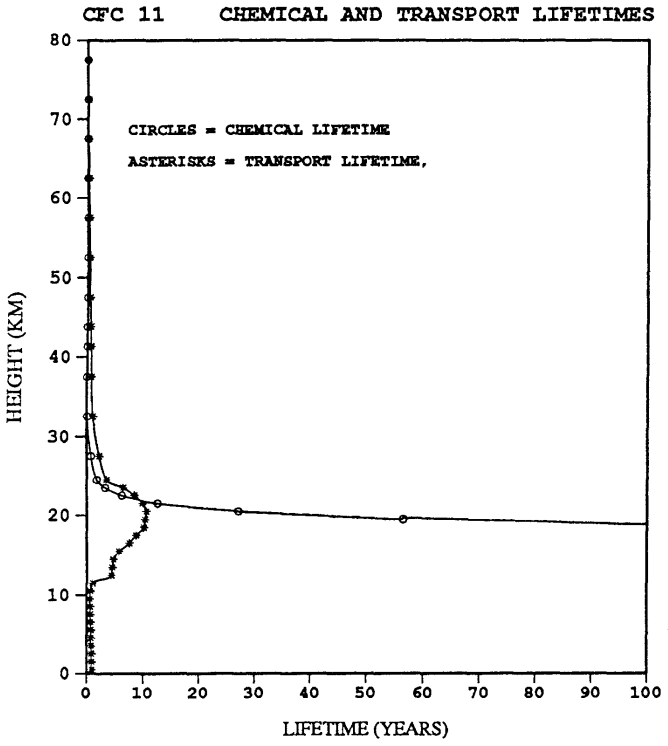

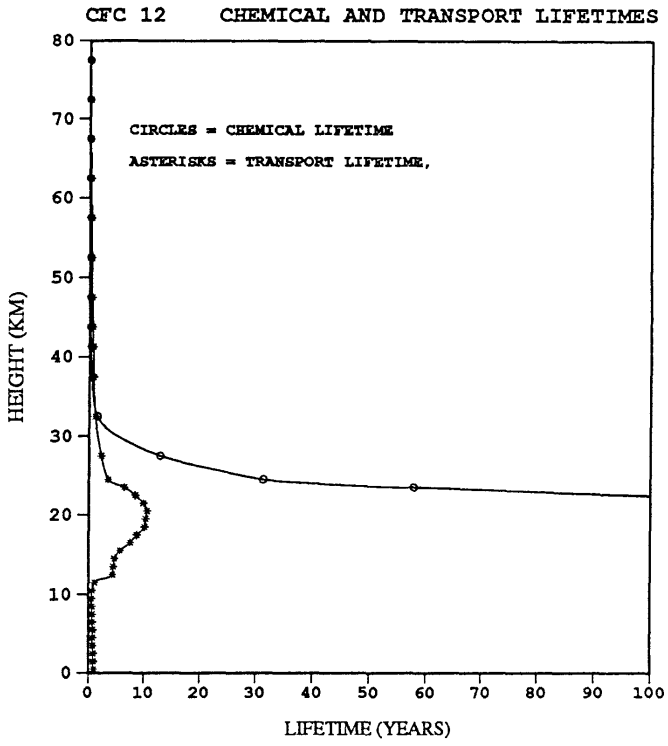

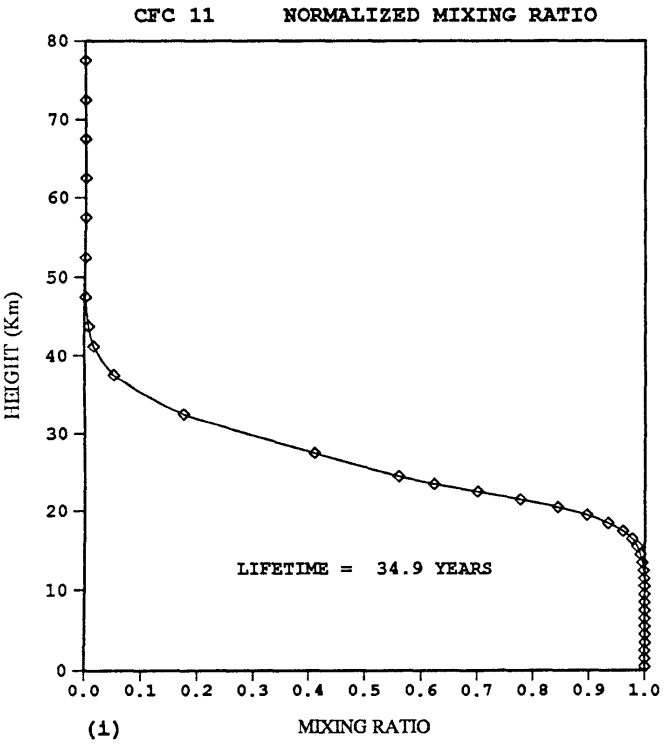

OH-HCFC RATE CONSTANT WAS TAKEN FROM JPL 1987 PUB.
30 DEGREES LATITUDE
CHANG AND DICKINSON'S K

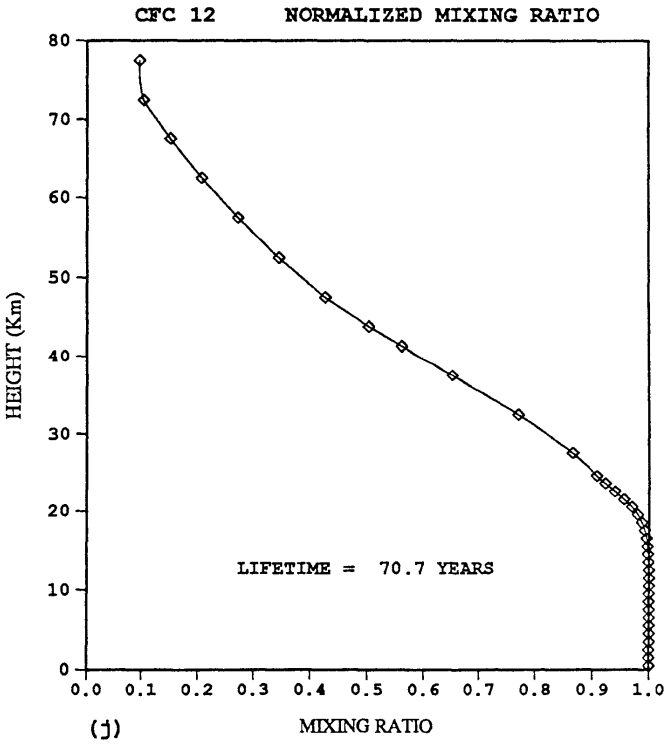

OH-HCFC RATE CONSTANT WAS TAKEN FROM JPL 1987 PUB.
30 DEGREES LATITUDE
CHANG AND DICKINSON'S K

FIGURE 3: cont'd.

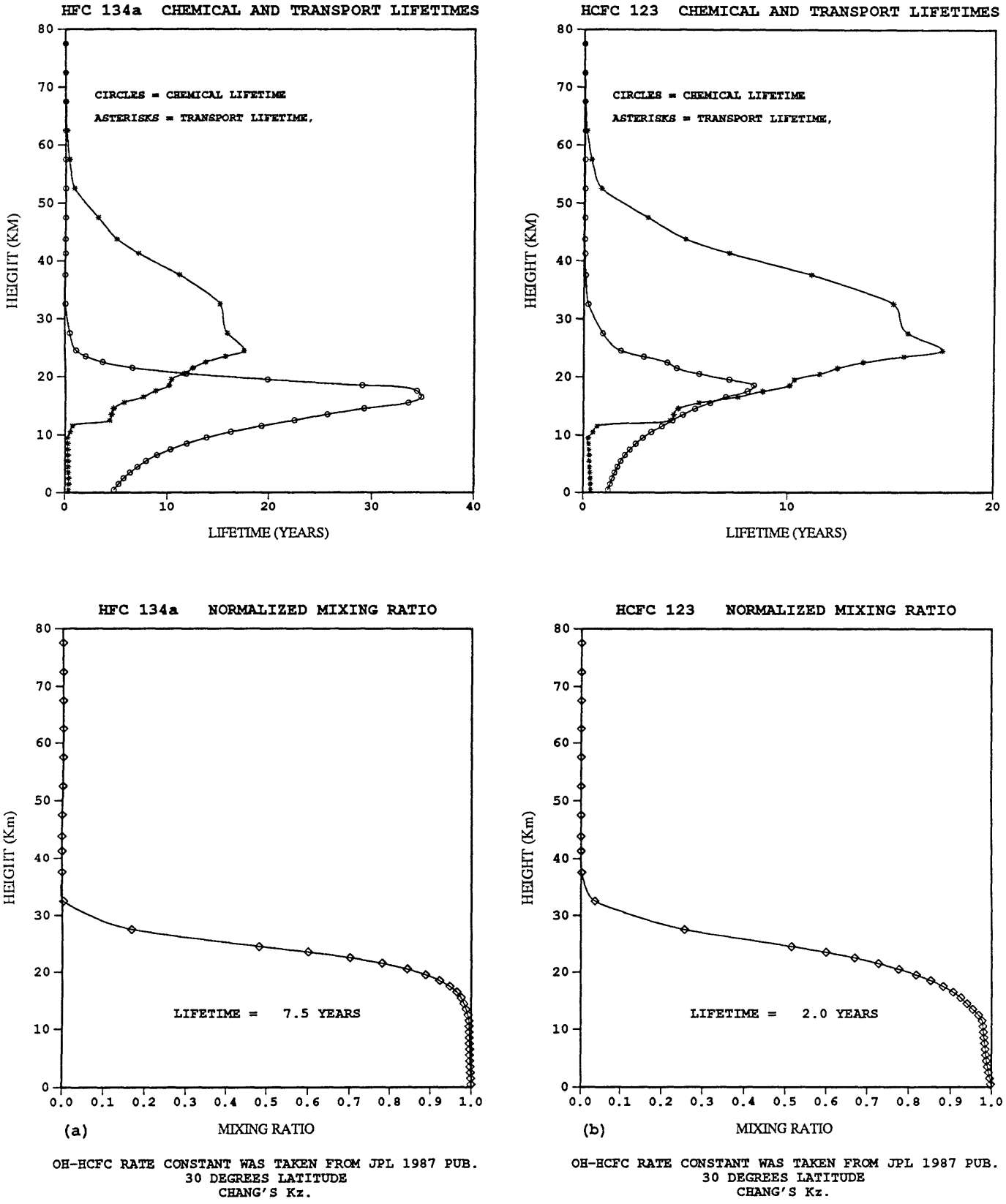

FIGURE 4: Same as in figure 2 but for the transport coefficient of Chang (1974).

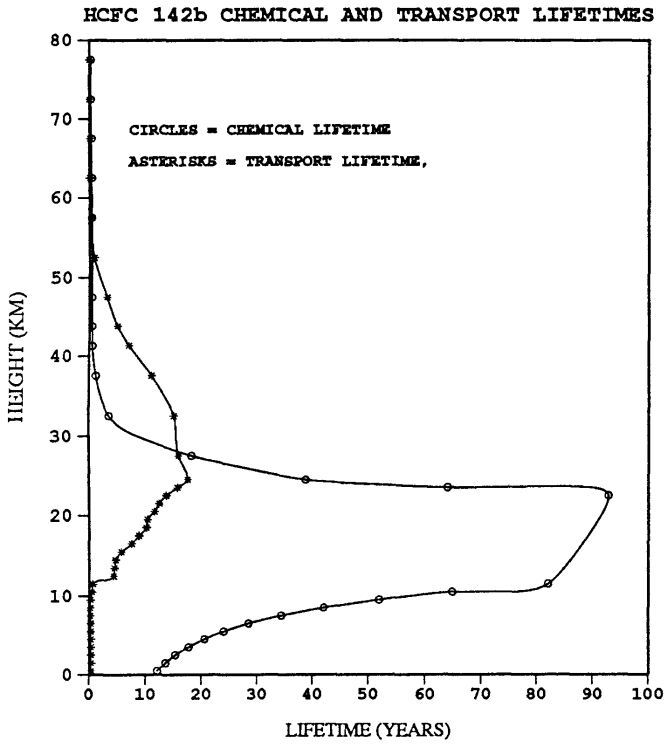

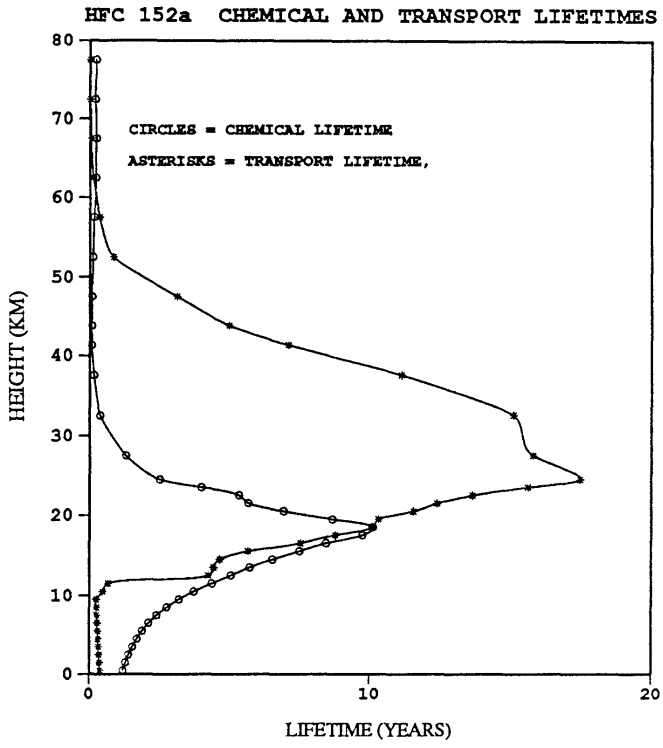

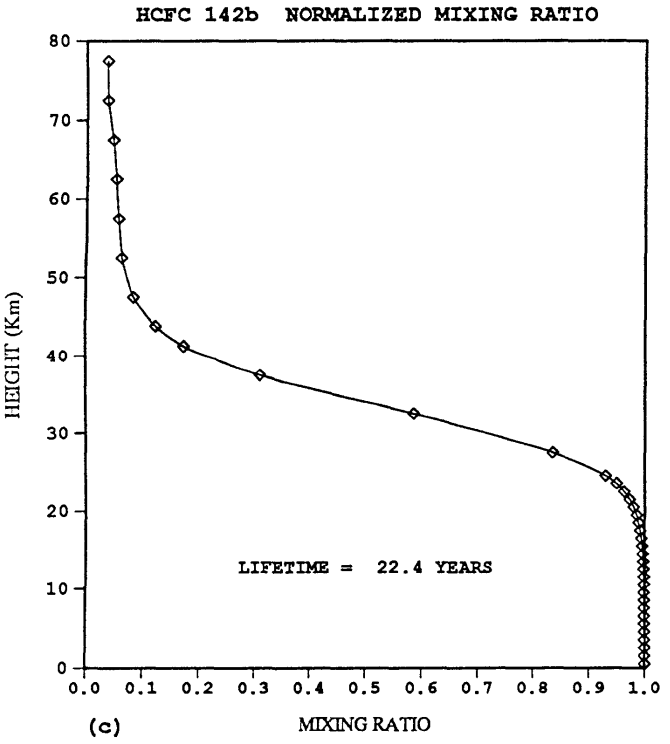

OH-HCFC RATE CONSTANT WAS TAKEN FROM JPL 1987 PUB.
30 DEGREES LATITUDE
CHANG'S Kz.

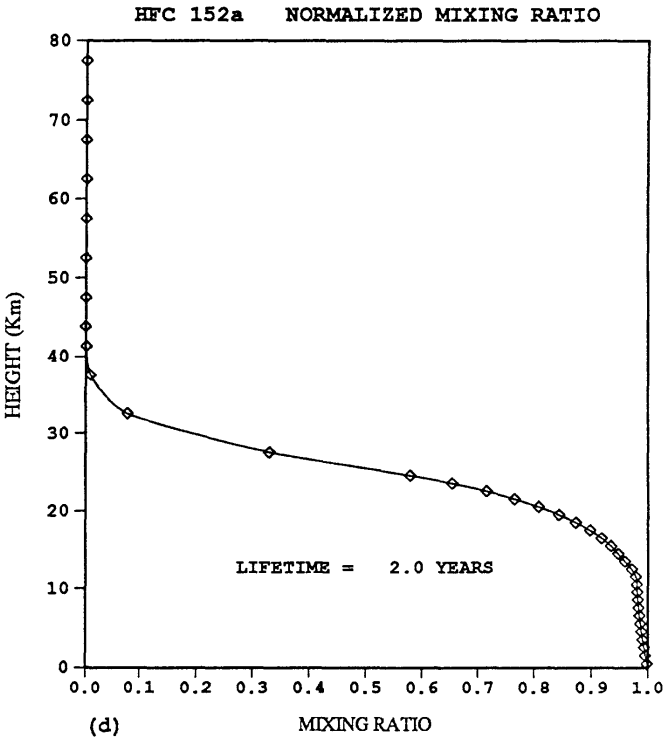

OH-HCFC RATE CONSTANT WAS TAKEN FROM JPL 1987 PUB.
30 DEGREES LATITUDE
CHANG'S Kz.

FIGURE 4: cont'd.

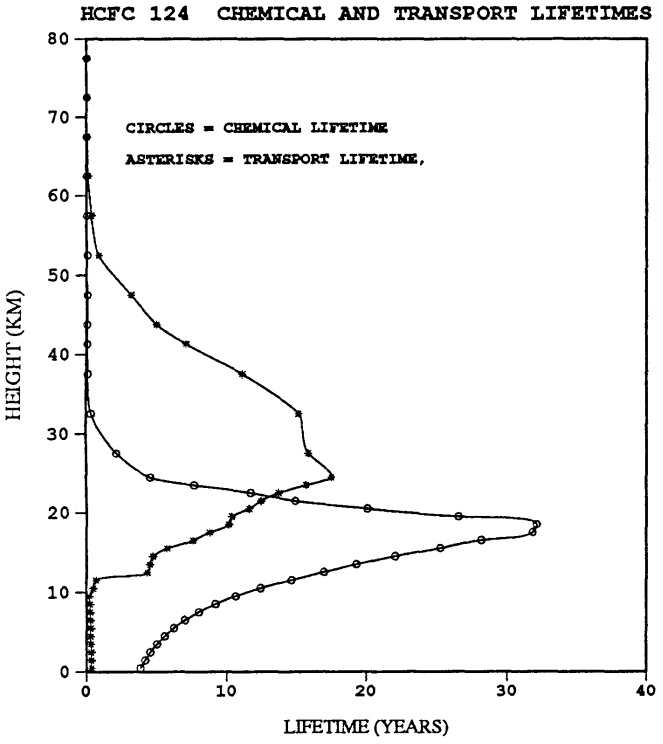

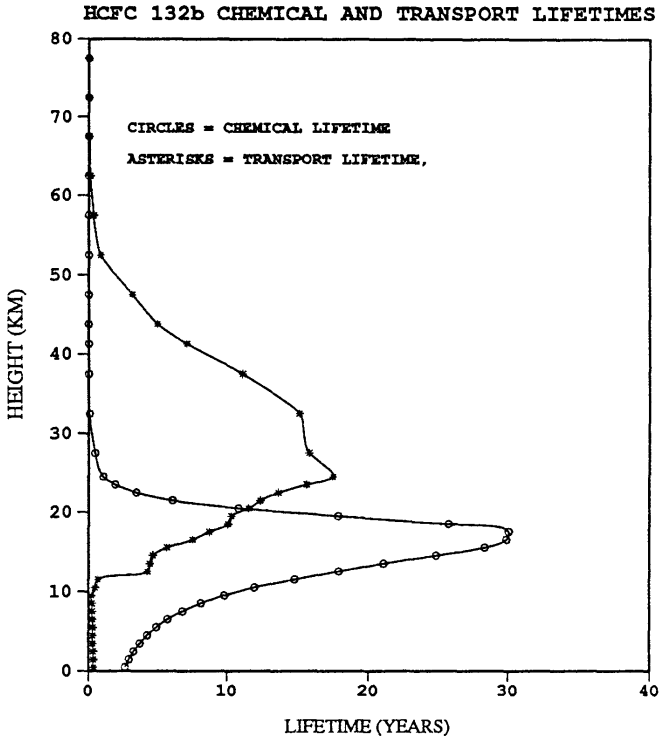

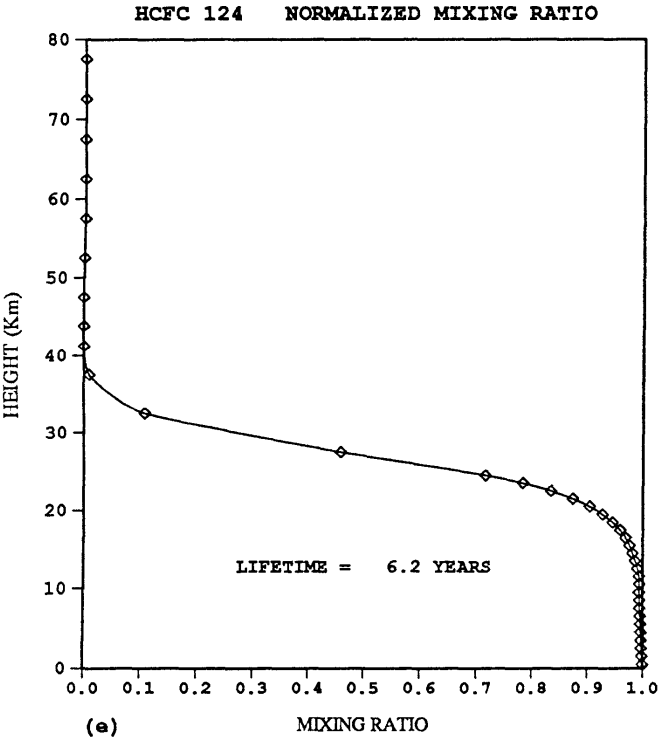

OH-HCFC RATE CONSTANT WAS TAKEN FROM JPL 1987 PUB.
30 DEGREES LATITUDE
CHANG'S Kz.

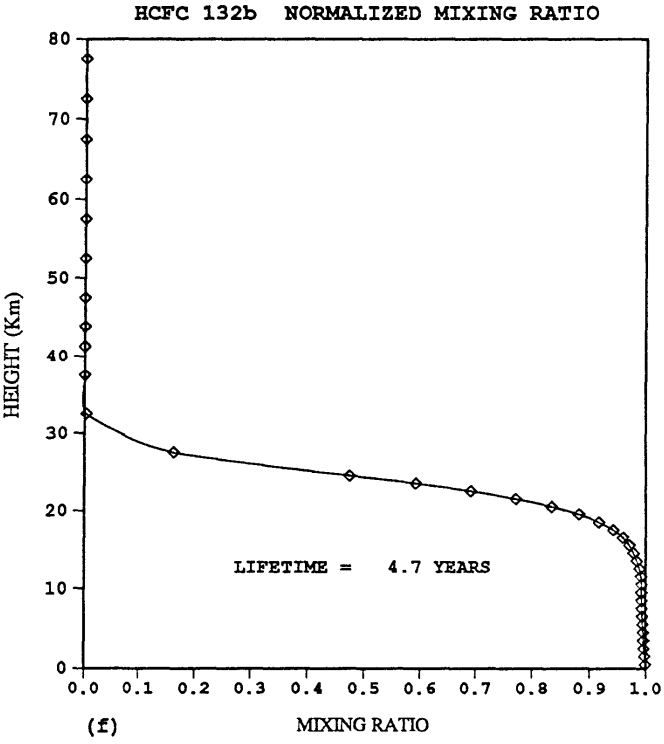

OH-HCFC RATE CONSTANT WAS TAKEN FROM JPL 1987 PUB.
30 DEGREES LATITUDE
CHANG'S Kz.

FIGURE 4: cont'd.

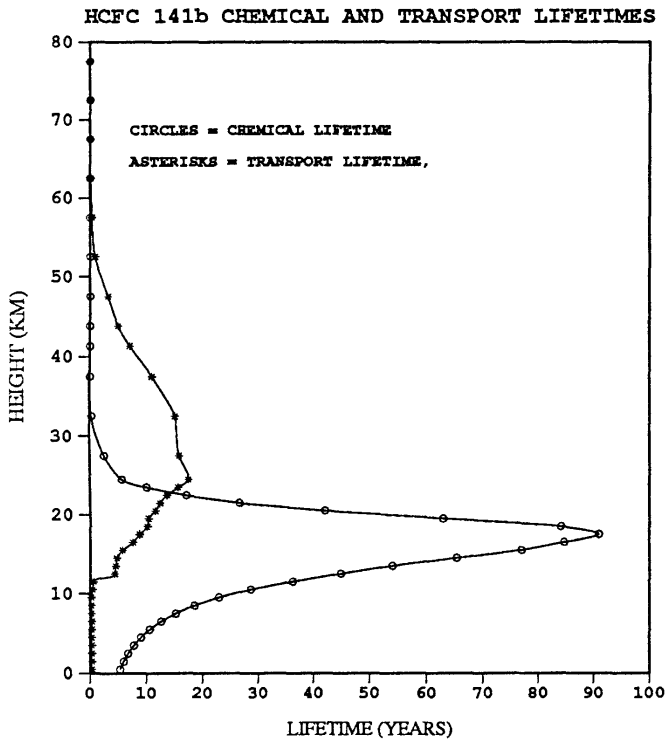

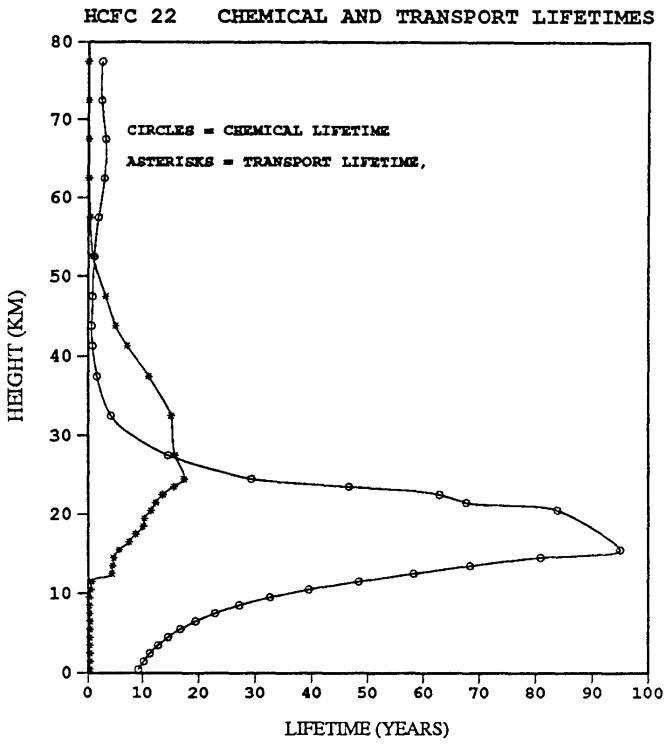

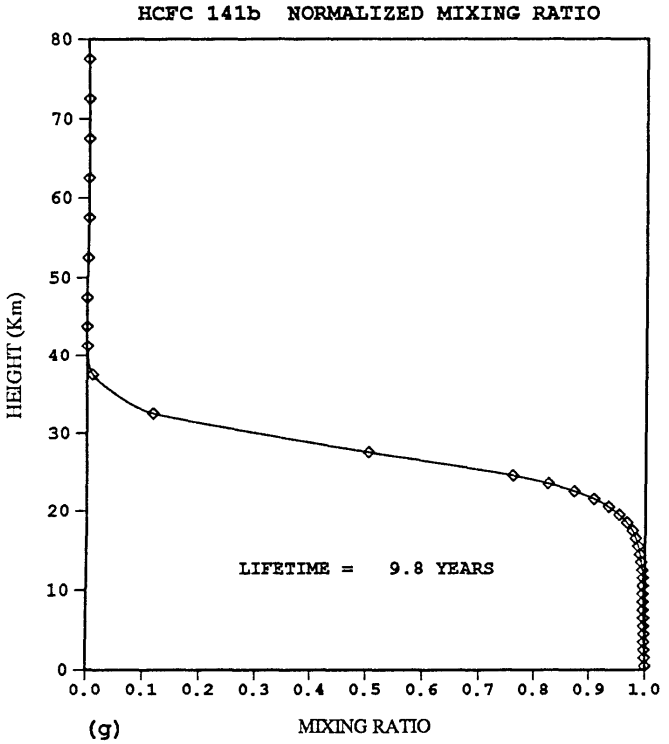

OH-HCFC RATE CONSTANT WAS TAKEN FROM JPL 1987 PUB.
30 DEGREES LATITUDE
CHANG'S Kz.

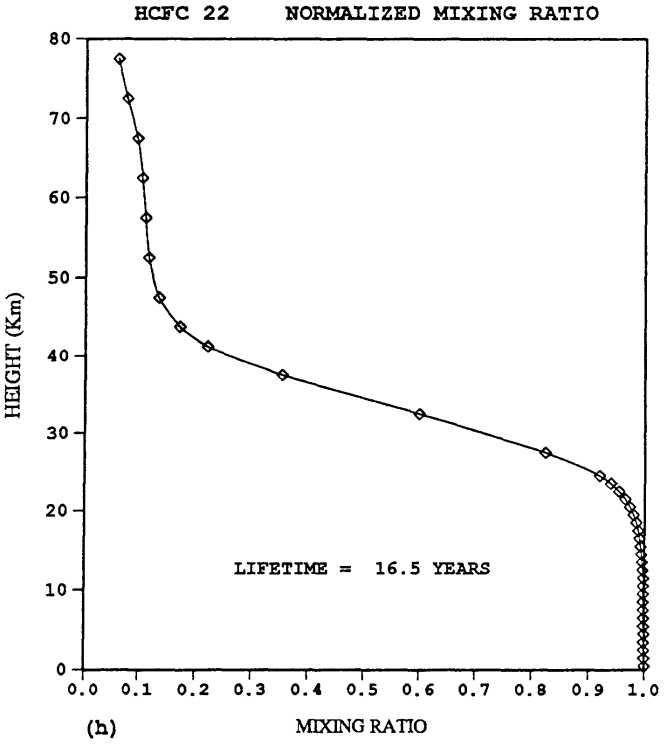

OH-HCFC RATE CONSTANT WAS TAKEN FROM JPL 1987 PUB.
30 DEGREES LATITUDE
CHANG'S Kz.

FIGURE 4: cont'd.

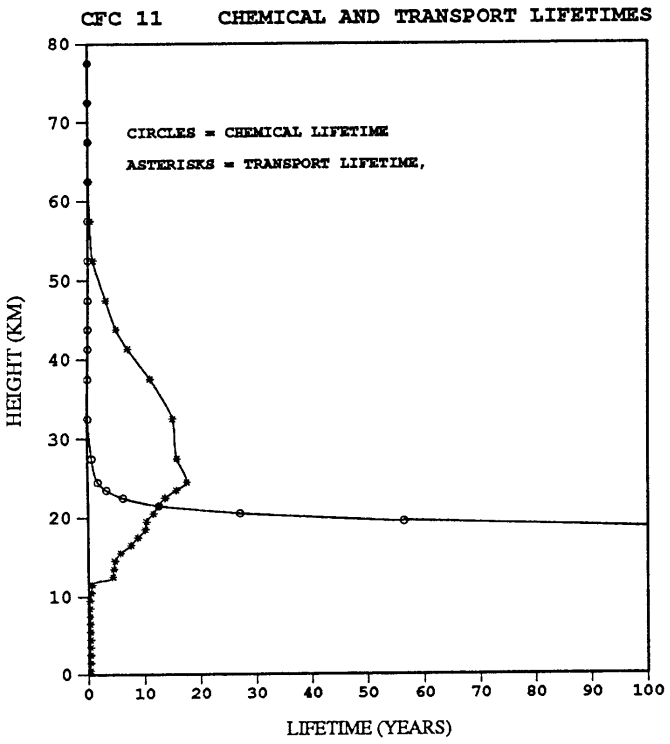

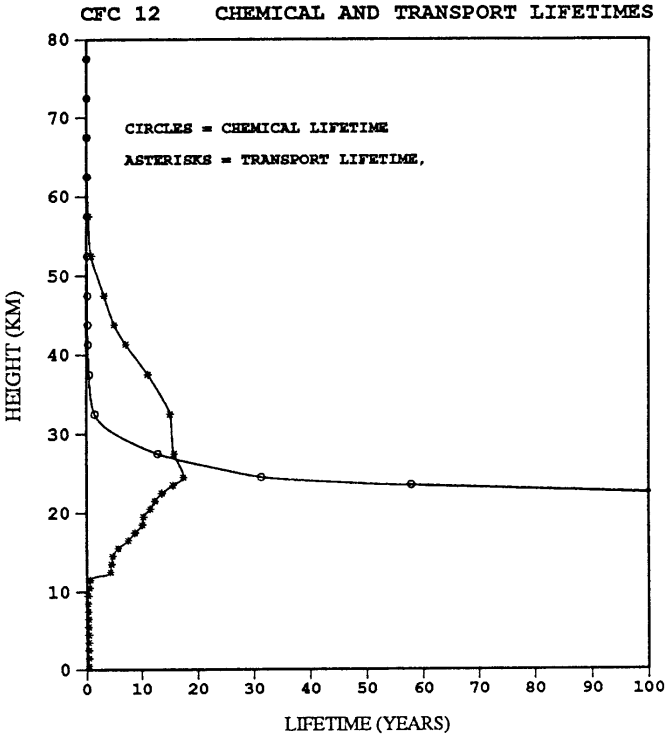

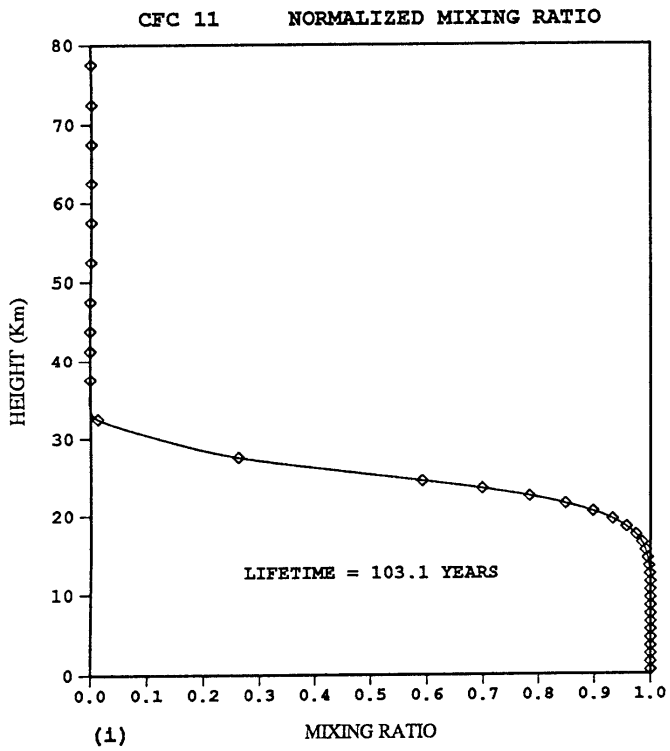

OH-HCFC RATE CONSTANT WAS TAKEN FROM JPL 1987 PUB.
30 DEGREES LATITUDE
CHANG'S Kz.

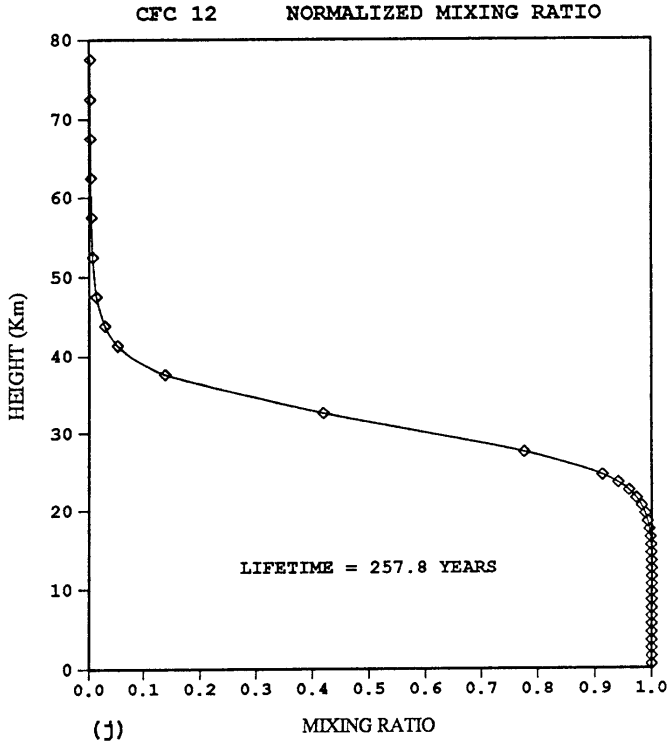

OH-HCFC RATE CONSTANT WAS TAKEN FROM JPL 1987 PUB.
30 DEGREES LATITUDE
CHANG'S Kz.

FIGURE 4: cont'd.

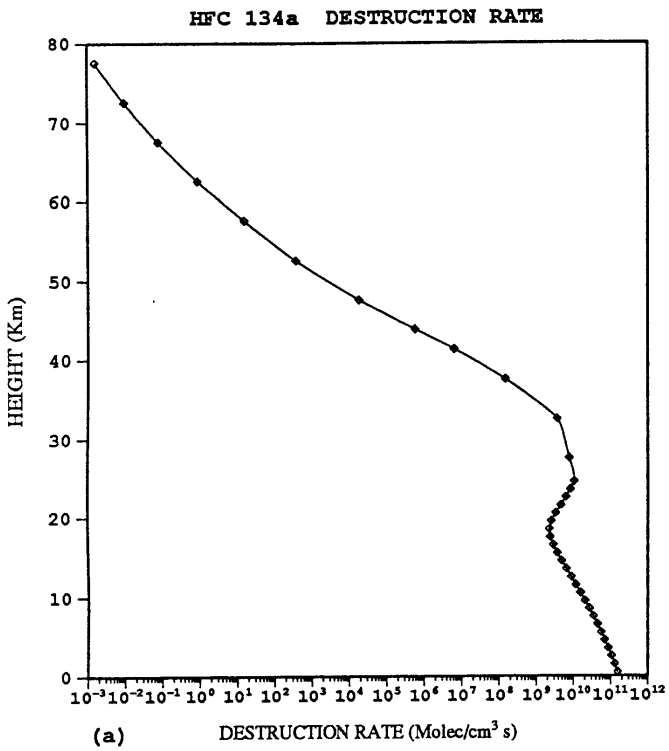

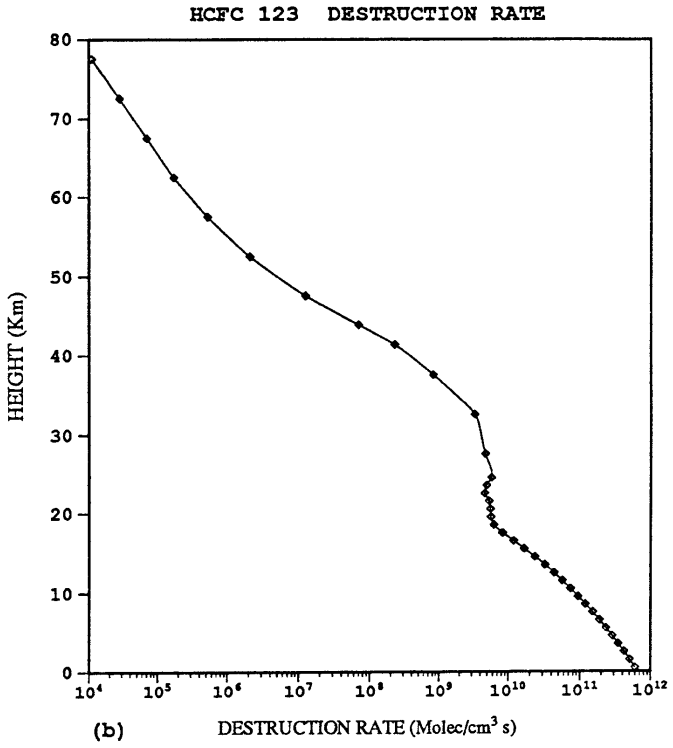

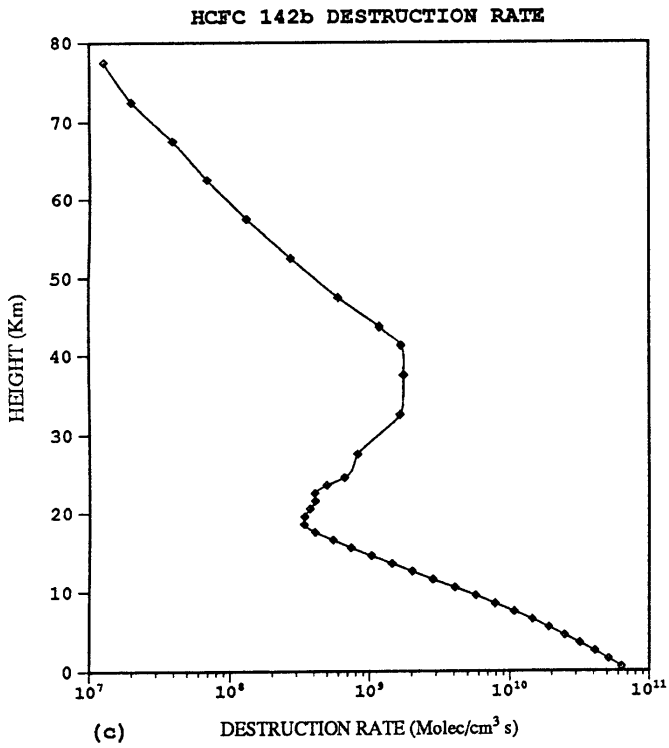

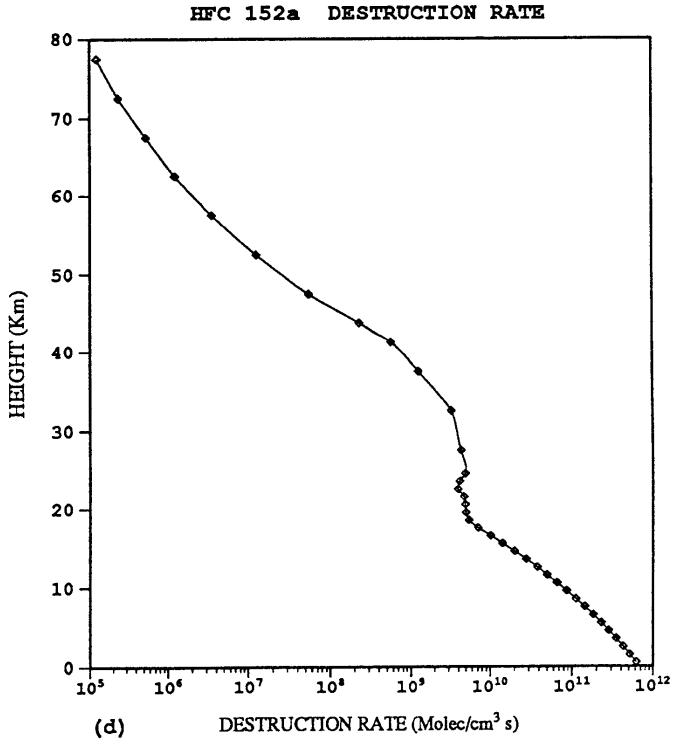

FIGURE 5: Model calculated rate of destruction versus height.

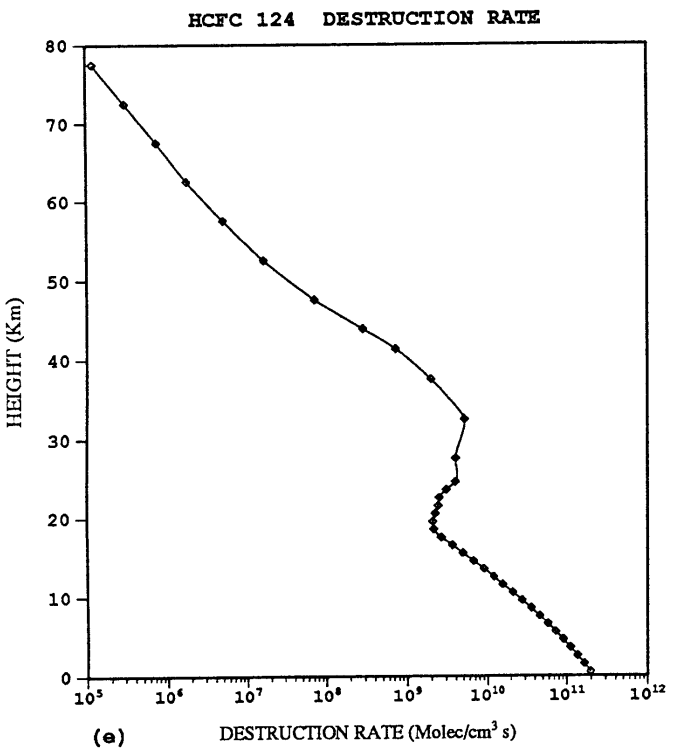

(e)

OH-HCFC RATE CONSTANT WAS TAKEN FROM JPL 1987 PUB.
30 DEGREES LATITUDE
HUNTEN'S Kz.

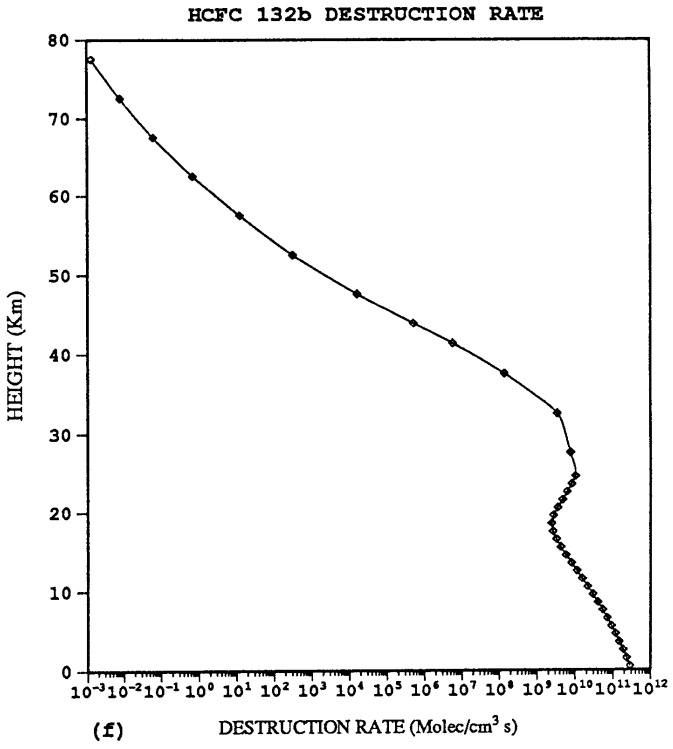

(f)

OH-HCFC RATE CONSTANT WAS TAKEN FROM JPL 1987 PUB.
30 DEGREES LATITUDE
HUNTEN'S Kz.

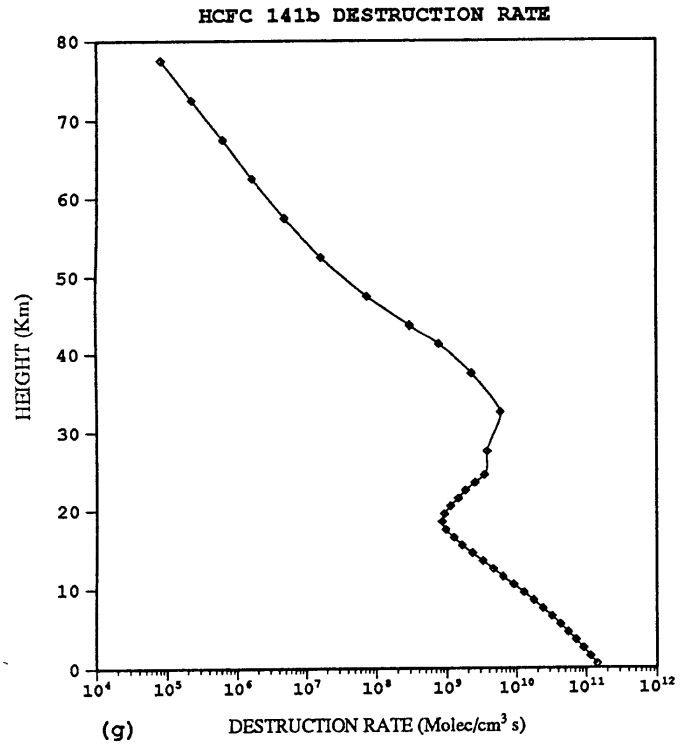

(g)

OH-HCFC RATE CONSTANT WAS TAKEN FROM JPL 1987 PUB.
30 DEGREES LATITUDE
HUNTEN'S Kz.

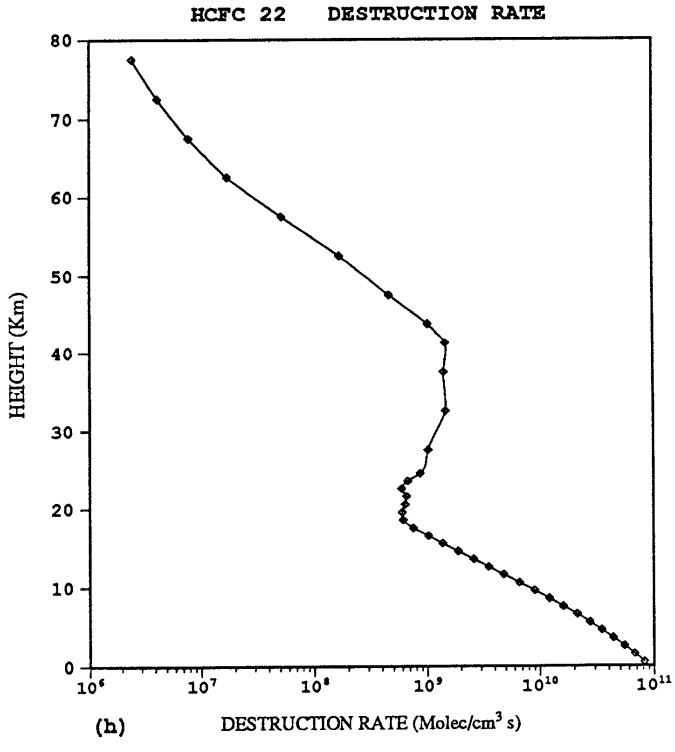

(h)

OH-HCFC RATE CONSTANT WAS TAKEN FROM JPL 1987 PUB.
30 DEGREES LATITUDE
HUNTEN'S Kz.

FIGURE 5 cont'd.

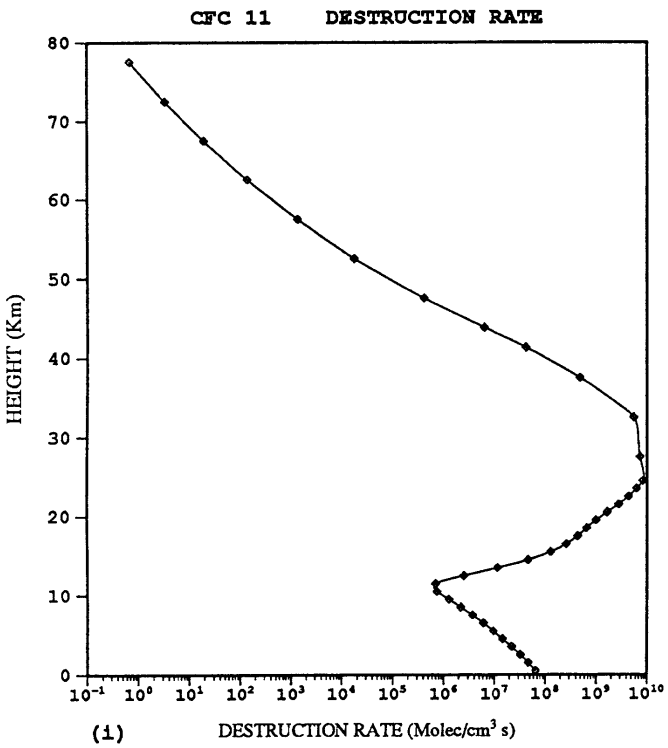

OH-HCFC RATE CONSTANT WAS TAKEN FROM JPL 1987 PUB.
30 DEGREES LATITUDE
HUNTEN'S Kz.

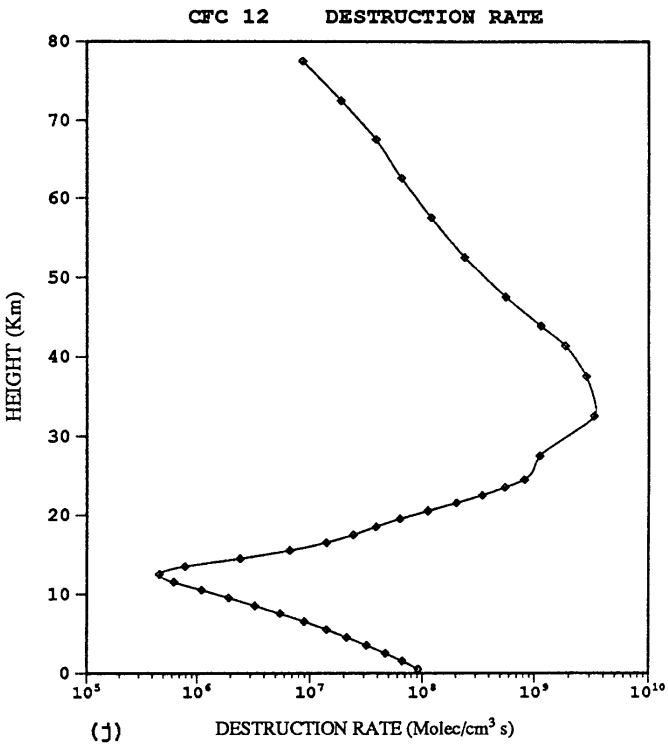

OH-HCFC RATE CONSTANT WAS TAKEN FROM JPL 1987 PUB.
30 DEGREES LATITUDE
HUNTEN'S Kz.

FIGURE 5 cont'd.

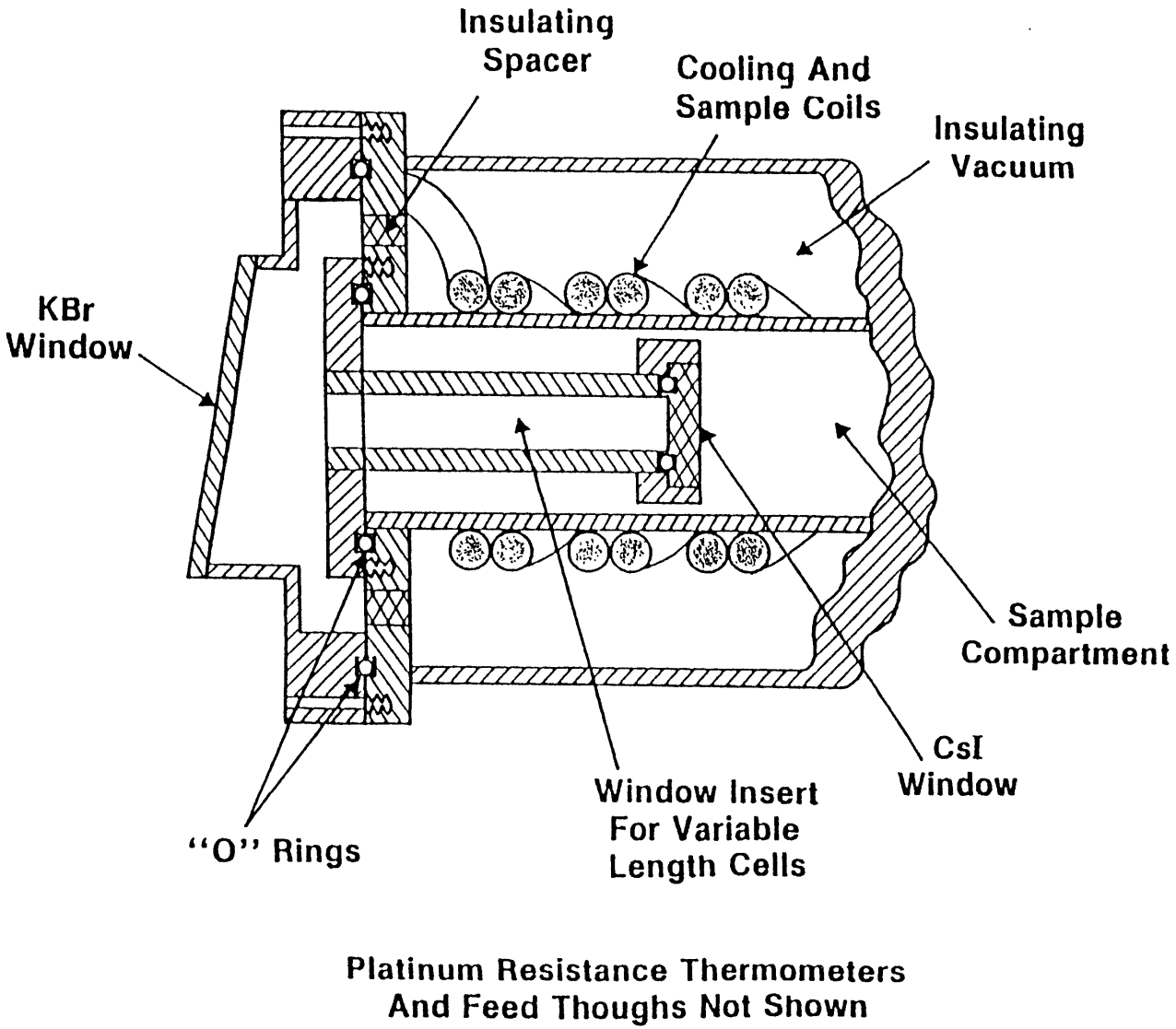

FIGURE 6: Cross-section for one end of the NBS cold cell.

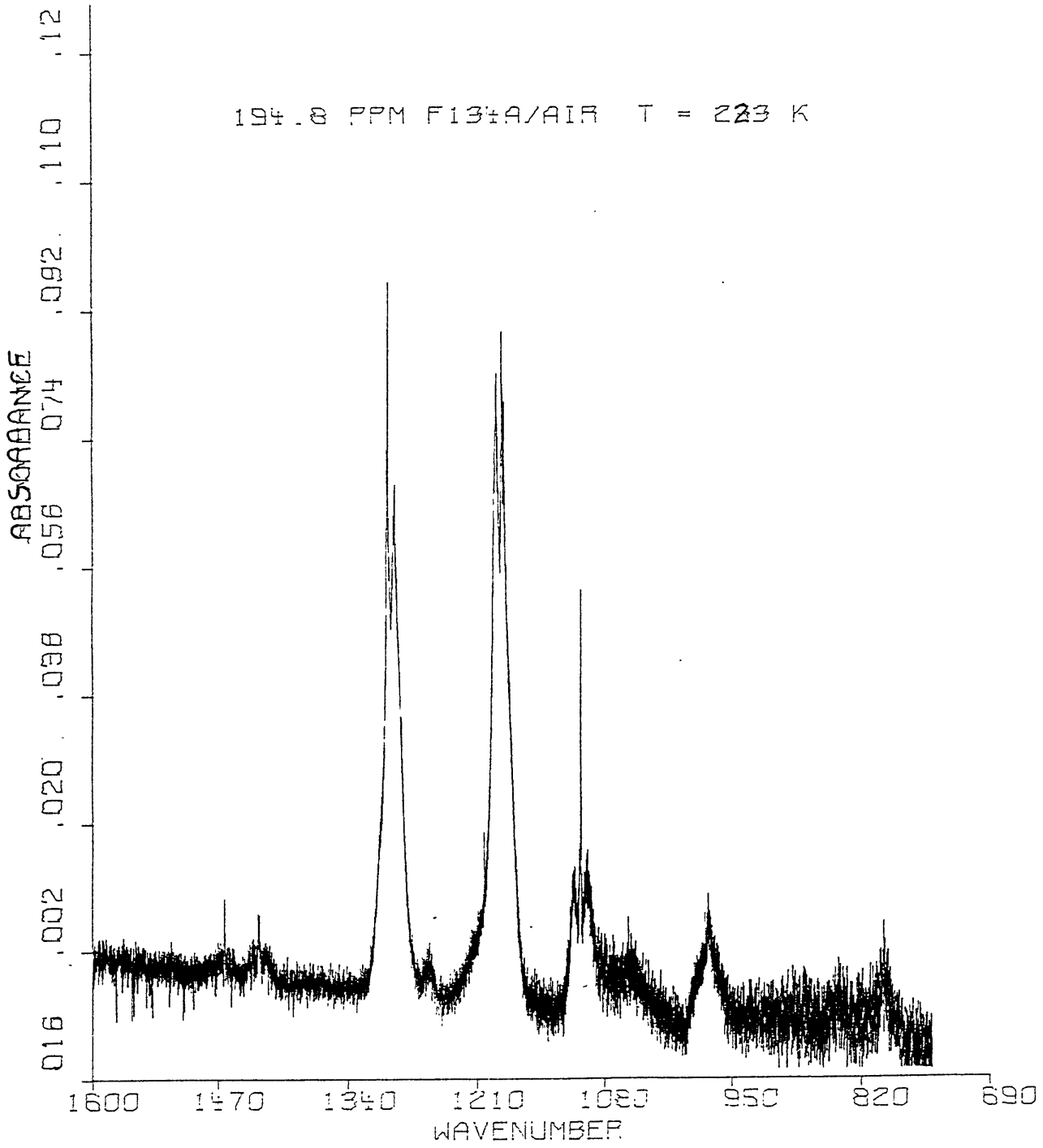

FIGURE 7a: The 194.8 ppm band system of CH_2FCF_3 at 223 K. Units on the vertical scale are log base 10 absorbance. Units on the horizontal scale are wavenumber (cm^{-1}).

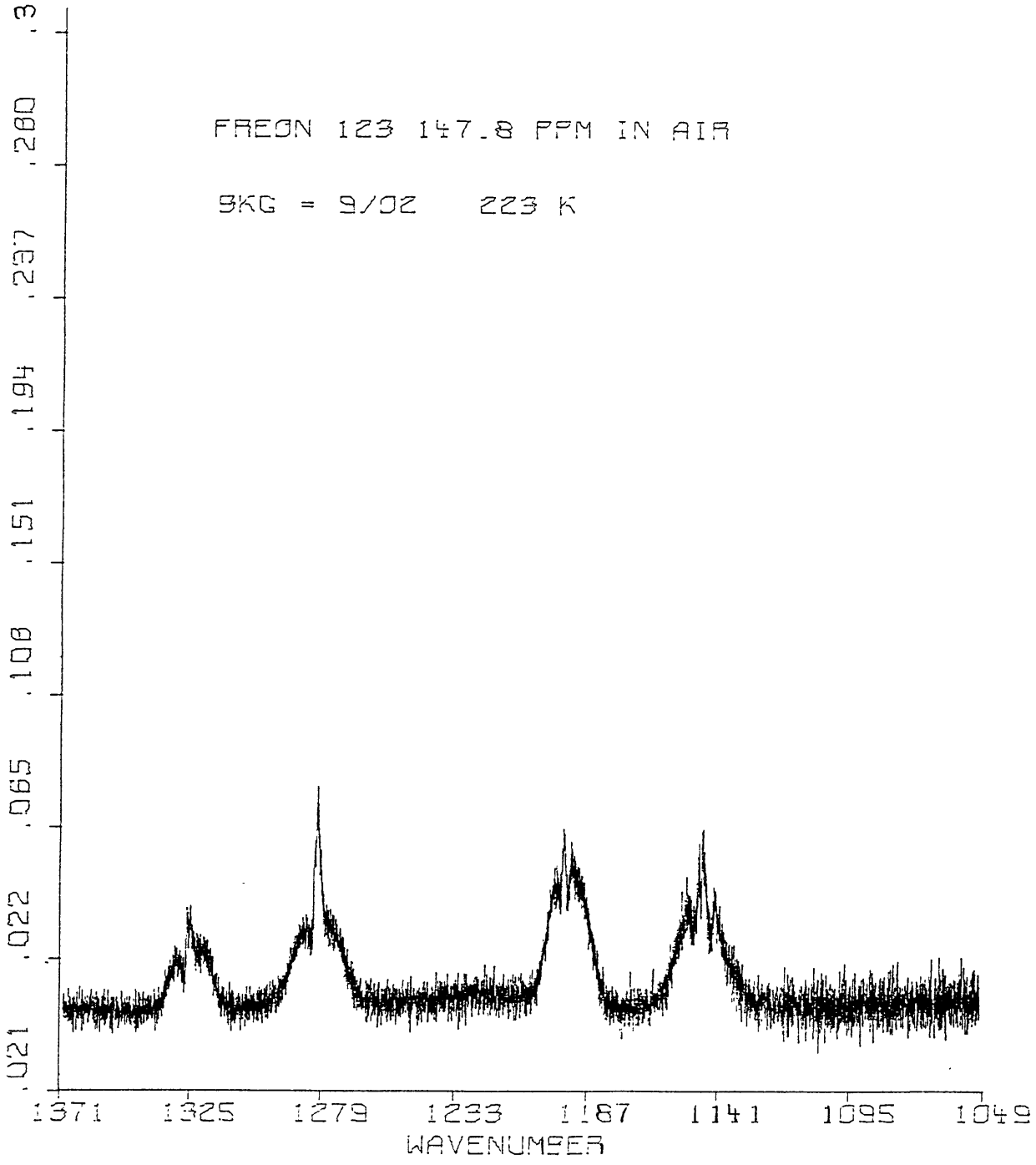

FIGURE 7b: The 147.8 ppm band system of $CHCl_2CF_3$ at 223 K. Units on the vertical scale are log base 10 absorbance. Units on the horizontal scale are wavenumbers (cm^{-1}).

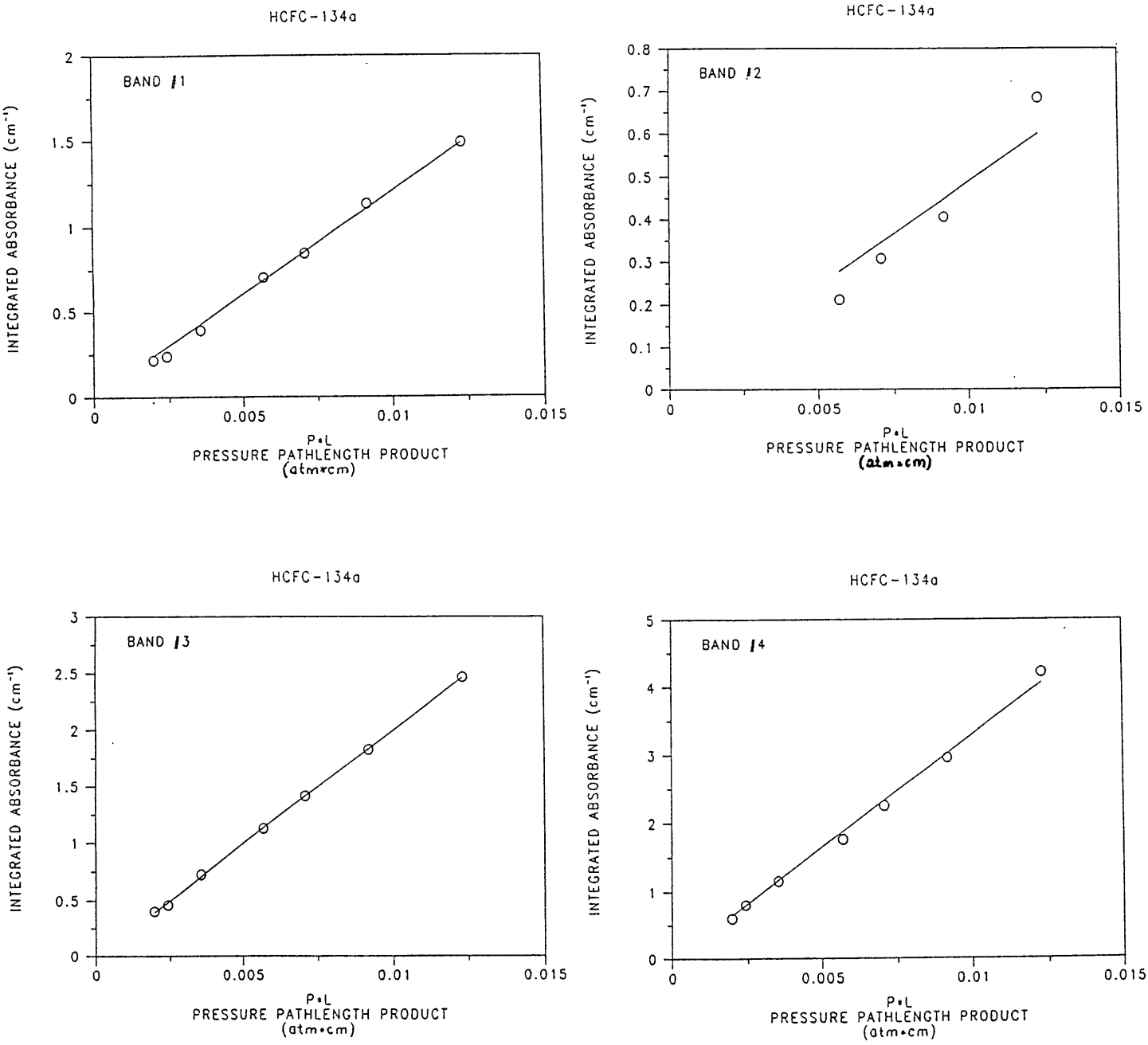

FIGURE 8: Beer's law plots of CH_2FCF_3 for the individual bands 1 through 6 and the total band system. Preliminary Data

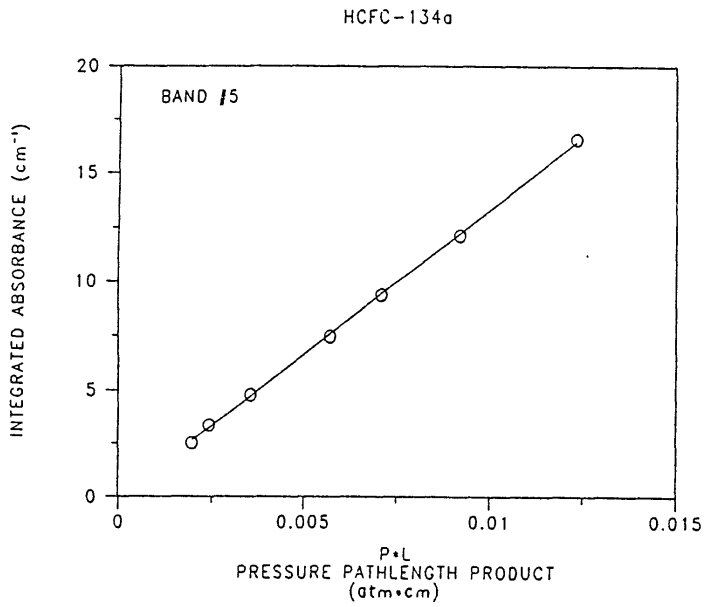

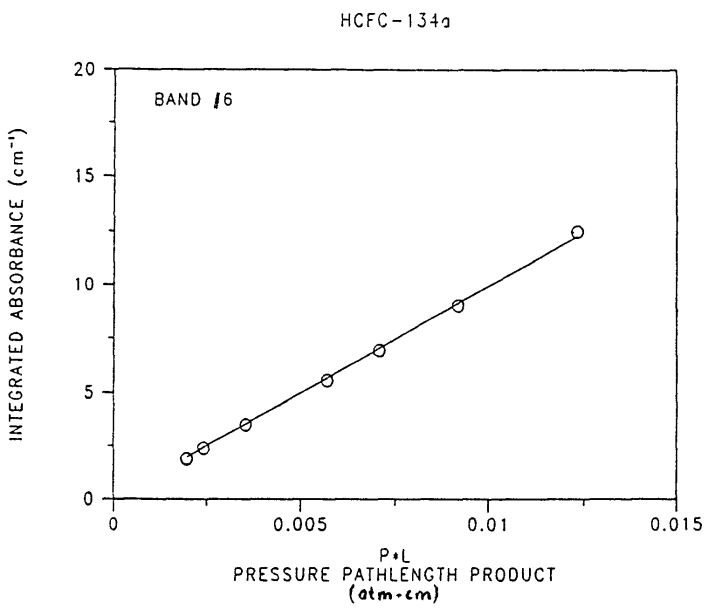

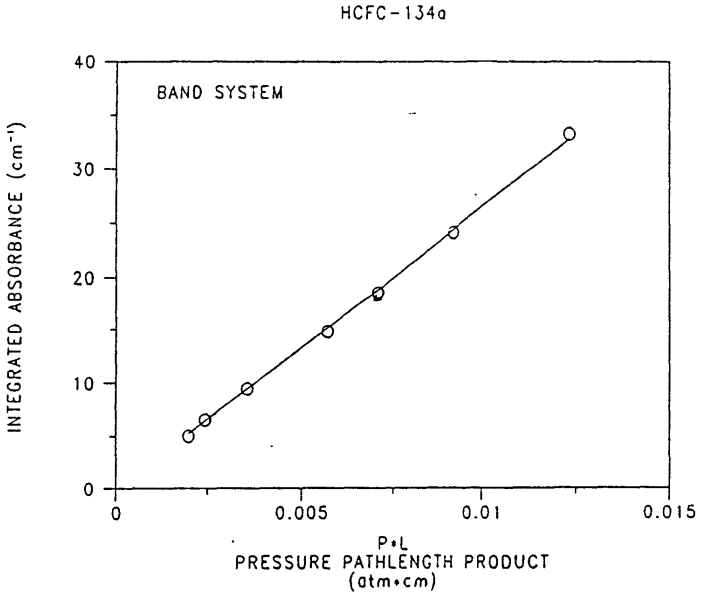

FIGURE 8 cont'd. Preliminary Data

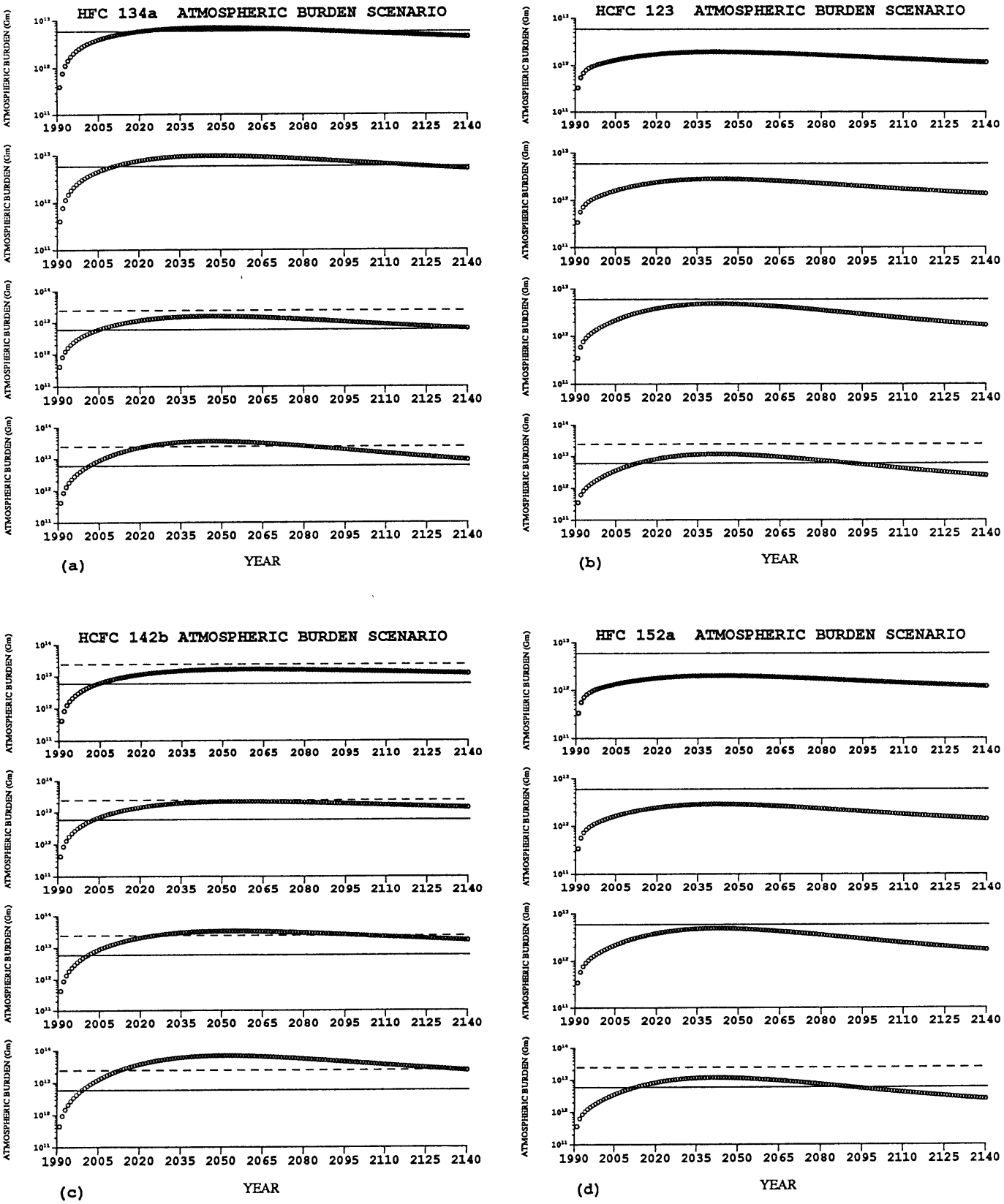

FIGURE 9: Emission scenarios for the substitute compounds using four different initial emission growth rates: 5%, 7%, 10%, 15%. The solid line shows the present atmospheric burden of F-11. The dashed line represents the Ramanathan et. al. (1985) radiative model levels.

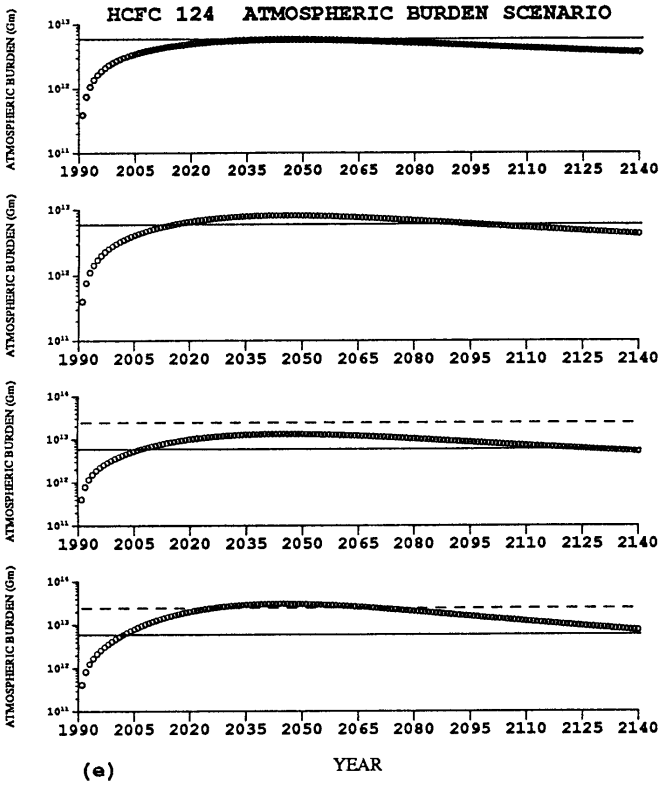

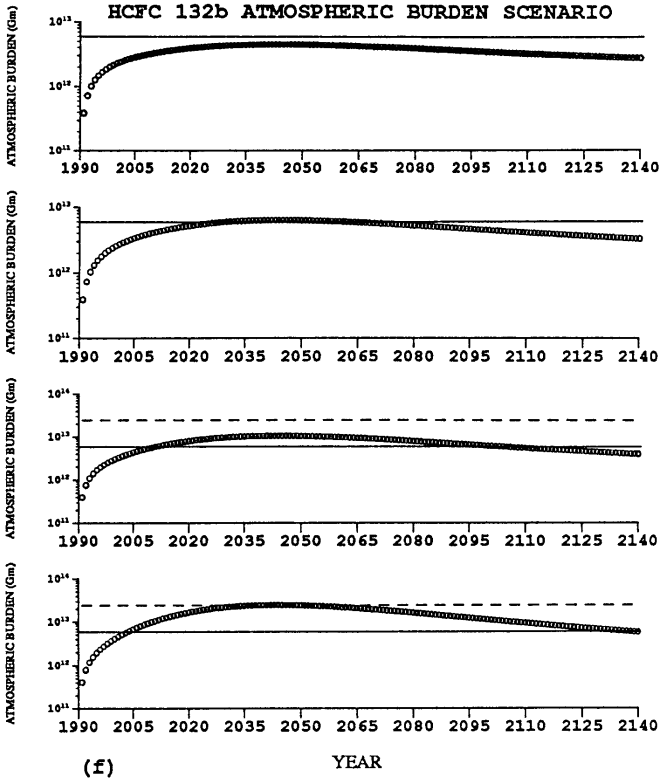

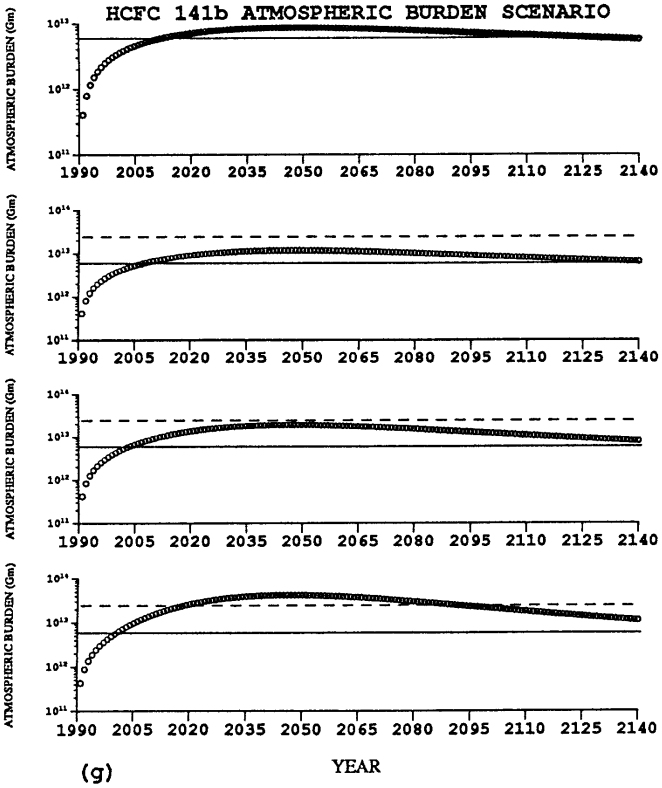

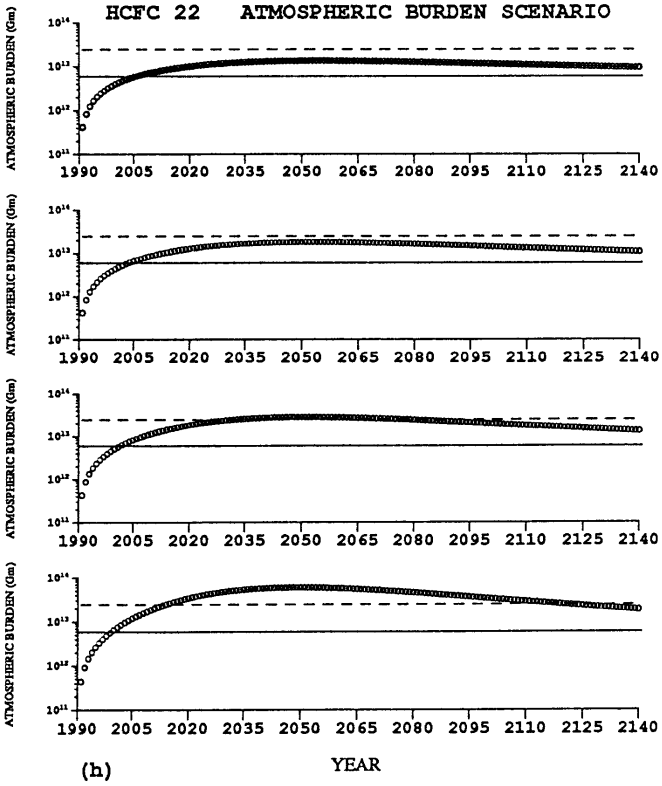

FIGURE 9 cont'd.

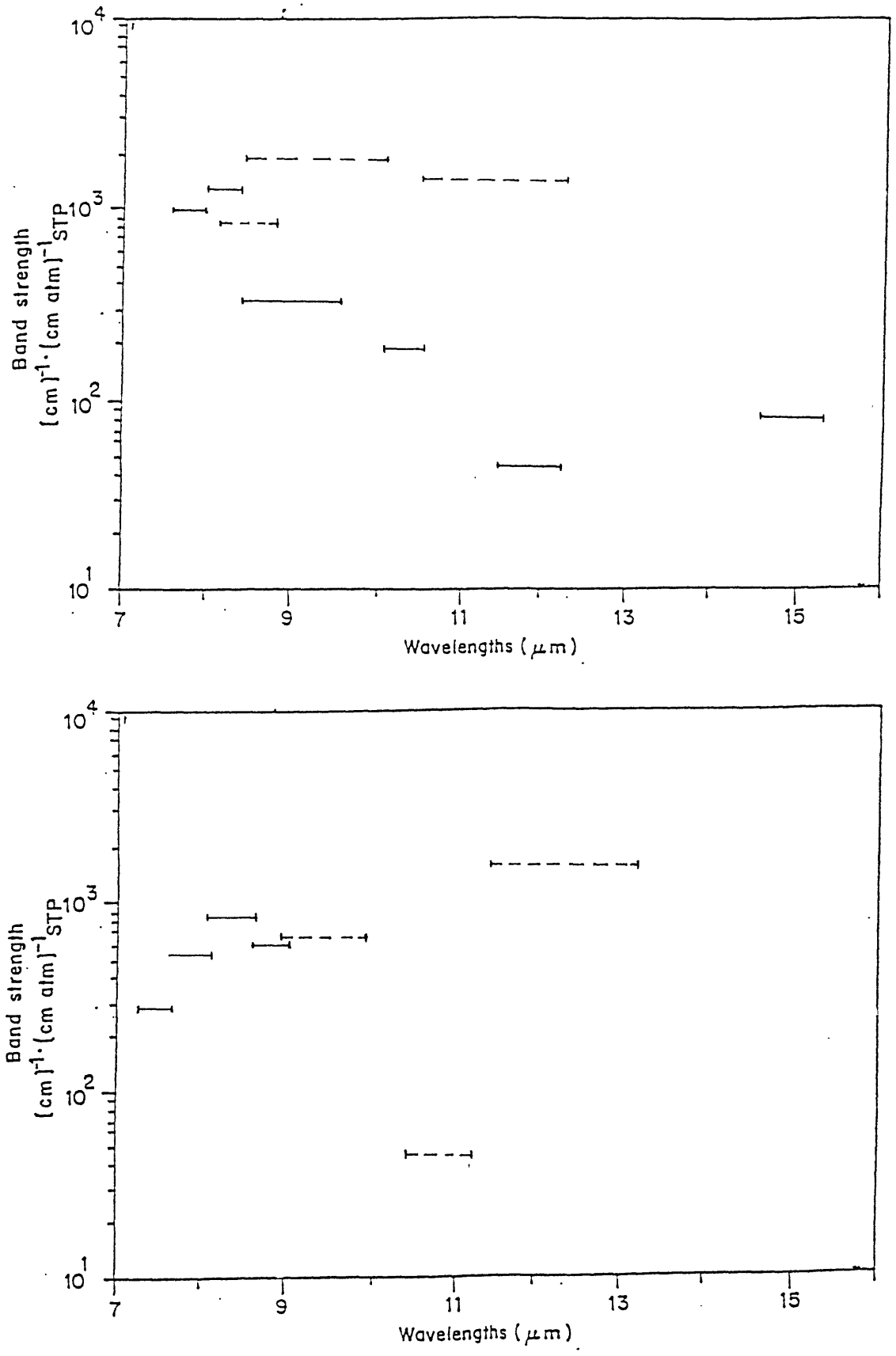

FIGURE 10: A comparison of the band intensity and spectral position of CCl_2F_2 versus CH_2FCF_3 (top panel) and CCl_3F versus $CHCl_2CF_3$ (bottom panel). Traditional CFC's are dashed lines and the substitutes are solid lines. The bounds of the 10 micron wondow are given.